



# 4D Treatment Planning Workshop 2015

7<sup>th</sup> international workshop for planning and  
delivery of radiotherapy to non-static targets

26-27 November 2015  
Dresden, Germany



**Hosted by OncoRay**

National Center for Radiation Research in Oncology  
Faculty of Medicine and University Hospital Carl Gustav Carus  
Technische Universität Dresden  
Helmholtz-Zentrum Dresden – Rossendorf  
Germany



## CONTACT

Christian Richter	<a href="mailto:christian.richter@oncoray.de">christian.richter@oncoray.de</a>
Kristin Stützer	<a href="mailto:kristin.stuetzer@oncoray.de">kristin.stuetzer@oncoray.de</a>
Antje-Christin Knopf	<a href="mailto:antje.knopf@icr.ac.uk">antje.knopf@icr.ac.uk</a>
Christoph Bert	<a href="mailto:christoph.bert@uk-erlangen.de">christoph.bert@uk-erlangen.de</a>

## PROGRAM

THURSDAY, 26 <sup>TH</sup> NOVEMBER 2015		
9:30	<b>Welcome Note</b>	Christian Richter
10:00-11:30	<b>Current Clinical Practice</b>	
	– Report on a survey on 12 particle therapy centers	Antje Knopf (ICR London)
	– Clinical point of view and general overview	Michael Baumann (OncoRay Dresden)
	– Practical experience and needs from a clinicians point of view	Stephanie Combs (TU München)
11:30-13:00	<b>Lunch</b>	
13:00-14:30	<b>4D + Robust Treatment Planning</b>	
	– What have commercial systems to offer – what do we need?	Francesca Albertini (PSI Villigen)
	– 4D Monte Carlo	Marcus Alber (Aarhus University)
	– Robust planning and margin concepts: What is the way to go?	Mischa Hoogeman (Erasmus MC Rotterdam)
14:30-17:00	<b>Coffee Break + Posters</b>	
17:00-17:30	<b>Motion Monitoring – IGRT – ART (I)</b>	
	– What can we learn from IGRT of photons?	Anne Richter (University Hospital Würzburg)
17:45-18:30	<b>Site Tour</b>	
19:30	<b>Conference Dinner</b>	

## PROGRAM

FRIDAY, 27<sup>TH</sup> NOVEMBER 2015

08:30-09:30 **Motion Monitoring – IGRT – ART (II)**

- |   |   |
|---|---|
| – Integration of new imaging capabilities in proton therapy | Toni Lomax<br>(PSI Villigen)            |
| – What is new in motion monitoring and motion modelling     | Guido Baroni<br>(Politecnico di Milano) |

09:30-10:00 **Coffee Break**

10:00-11:30 **Motion Modelling and Deformable Registration**

- |  |  |
|--|--|
| – New developments and improvements in DIR                               | Hugo Furtado<br>(Medical University of Vienna) |
| – Relating motion to external surrogates                                 | Daniel Low<br>(UCLA)                           |
| – How to verify DIR? Can we use DIR in the clinic and for which purpose? | Dave Hawkes<br>(University College London)     |

11:30-13:00 **Lunch**

13:00-14:30 **4D Dosimetry**

- |  |  |
|--|--|
| – Overview <i>in vivo</i> verification including 4D capabilities       | Wolfgang Enghardt<br>(OncoRay Dresden) |
| – 4D simulation of secondary emissions for <i>in vivo</i> verification | Katia Parodi<br>(LMU Munich)           |
| – Prompt-Gamma techniques and its 4D capabilities                      | Guntram Pausch<br>(OncoRay Dresden)    |

14:30-14:45 **Coffee Break**

14:45-15:45 **Panel Discussion**

15:45-16:00 **Summary**

Report, Poster award, Location & focus next year

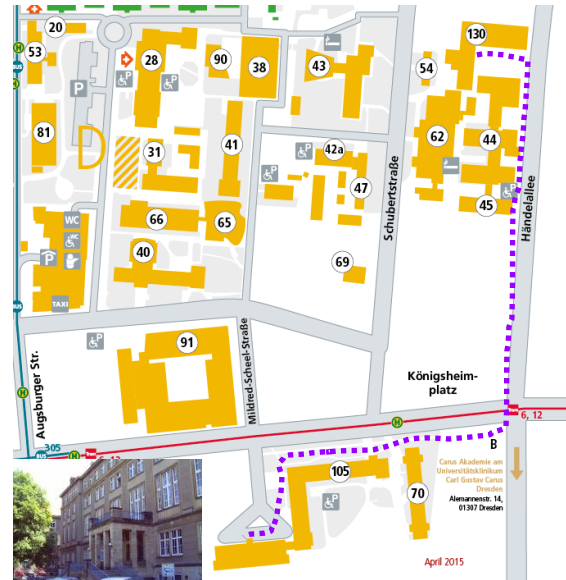
## WHERE TO GO FOR ...

### ... LUNCH?

We will have our lunch on Thursday and Friday at the refectory / canteen of the Medical Faculty Carl Gustav Carus of the Technische Universität Dresden.

It is a 5-10 min walk away from the OncoRay (see map).

**Don't forget your vouchers!**



### ... DINNER?

We invite you to join the dinner on Thursday evening in the center of Dresden. The restaurant *Italienisches Dörfchen* (Theaterplatz 3, 01067 Dresden) is located next to the Semperoper and the river Elbe.



For the direct route from the OncoRay to the restaurant take at station Königsheimplatz the tram No 12 with final destination Leutewitz. After about 15-20 min, disembark at station Postplatz. From there it is a short walk passing the Zwinger, Semperoper and Hofkirche.



# ROUTE MAPS FOR PUBLIC TRANSPORT





**Tarifzone 61**  
Fretal

## POSTER PRESENTATIONS

### 4D DOSE CALCULATIONS AND DOSIMETRIC ANALYSES PAGE

1) 4D-Optimization to Counter Inter- and Intrafractional Motion in Scanned Ion Beam Lung Cancer Therapy	10
2) Pencil beam scanning proton therapy of lung cancer: Impact of interplay effect	11
3) Quantification of interplay effects of PBS-based lung tumour treatments under various fractionation schemes with/without rescanning: the Varian ProBeam experiences	12
4) Limited impact of breathing motion, interplay effect and set-up/range uncertainties in IMPT for advanced stage NSCLC	14
5) Planning studies for non-invasive treatment of cardiac arrhythmias with scanned carbon ion beams	15
6) Changing from ITV to MidV concept – Do we have to adapt the prescribed dose?	16
7) A strategy for robust radiotherapy treatment plans for pre-operative oesophageal cancer	17
8) Validation of a tool for monitoring inter-fractional anatomical changes in abdominal patients	18
9) Influence of organ motion on relative risks of radiation-induced secondary cancer for VMAT and IMPT of prostate cancer	20
10) Investigation of magnetic field and motion effects on IMRT dose delivery using Monte Carlo simulations	21

### CLINICAL APPLICATIONS PAGE

11) Initial clinical experience of spot-scanning proton beam therapy using real-time-image gated proton-beam therapy system	23
12) Efficacy assessment of abdominal compression in 4DCT	24
13) Respiratory gating guided by internal electromagnetic motion monitoring during stereotactic radiation therapy in the liver	25
14) Treatment of liver tumors close to the skin surface with real-time image gated, spot-scanning proton beam therapy (RGPT) system – comparison between range compensation devices	26

### 4D IMAGING PAGE

15) New prospective and practical 4DCT	27
16) Comparison of 4DCT retrospective reconstruction with two different motion monitoring systems	29
17) Evaluation of differences in the target displacement between X-ray fluoroscopic and four-dimensional cone-beam computed tomography imaging with amplitude- and phase-based sorting	30

## POSTER PRESENTATIONS

<b>MEASUREMENTS AND PHANTOM STUDIES</b>		<b>PAGE</b>
18)	Real time tracking by CyberKnife and Vero in liver SBRT: dosimetric comparison by planning structure-based $\gamma$ -evaluation and dose-area-histograms	31
19)	Monitoring of respiratory motion: comparative analysis of optical and electromagnetic solutions	32
20)	Geometric and dosimetric validation of motion monitoring techniques in respiratory-gated radiotherapy using a dynamic lung phantom in combination with dosimetry gels	33
21)	A comparison of proton PBS and photon VMAT treatments with film dosimetry in the anthropomorphic lung phantom (LuCa)	34
22)	Measurements and simulations of charged secondary production in view of pre-clinical tests of in-vivo monitoring system for ion beam therapy	36
<b>MOTION ACQUISITION BY ULTRASOUND AND MOTION MODELLING</b>		<b>PAGE</b>
23)	Real-time Tracking of Liver Landmarks in 2D Ultrasound Sequences	37
24)	Ultrasound and MR-Tracking for Intra-Fractional Motion Compensation in Radiation Therapy	38
25)	The 2015 Challenge on Liver Ultrasound Tracking	39
26)	Estimation of tracking confidence and its use for gated-tracking	40
27)	Liver-Rib Motion Model for Predicting Rib Motion during Free-Breathing	41
28)	Prediction of respiratory liver motion via robust exemplar model and individualization from an additional breath-hold image	42
29)	Respiratory Motion Compensation with Topology Independent Surrogates	43
<b>DATABASES</b>		<b>PAGE</b>
30)	A Tool for an Interactive Summary of a Radiotherapy Treatment	44
31)	Compilation of a repeat 4D image database – concept and call for data	45

## 4D DOSE CALCULATIONS AND DOSIMETRIC ANALYSES

### 1) 4D-Optimization to Counter Inter- and Intrafractional Motion in Scanned Ion Beam Lung Cancer Therapy

C. Graeff, M. Durante

GSI Darmstadt

**Background:** 4D-optimization takes into account all 4DCT phases to incorporate motion and range changes. The resulting 4D-treatment plans require a delivery synchronized to the patient's motion. Here, we address the question whether 4D-optimization is feasible also with variable breathing motion, by planning on one 4DCT and simulated delivery on serial 4DCTs.

**Material and Methods:** For 4 patients, in total 6 weekly 4DCTs were available, so that 5 fractions could be simulated with a total dose of 47 Gy (RBE) corresponding to a BED of 120 Gy ( $a/b = 6\text{Gy}$ ). Calculations were performed with GSI's TRiP4D and LEM IV.

4D-plans were optimized on the baseline CT, delivering a uniform dose to each motion phase. In this strategy (4D-rescanning), no gradients occur between phases resulting in an inherent rescanning effect. In addition, vector fields from deformable image registration were not necessary for the optimization, but for contour propagation and later forward dose calculation. Doses were calculated for each fraction and accumulated on the baseline end-exhale phase. Isotropic margins of 0, 3, 5 and 7 mm as well as field-specific range margins of 0, 2, 3 %/mm H<sub>2</sub>O were investigated. For comparison, a range ITV plan was computed for selected margins. Delivery was assumed to be perfectly synchronized; for the ITV plans each phase received 10% of the dose to eliminate interplay. Dose coverage was assessed by V95, with 95% assumed as clinically acceptable. Conformity index (CI) and homogeneity (D5-D95) as well as Lung V20 were compared between 4D and ITV plans.

**Results:** Patient characteristics are shown in Table 1. For all patient, V95 > 95% could be achieved both in each fraction and total treatment, but with strongly varying margin size. In comparison to the ITV irradiations, CI and Lung V20 were always superior for the same margins.

**Conclusion:** 4D-optimization is feasible also for a time series of 4DCTs similar to a clinical situation. It offers better conformity than an ITV strategy, but might further benefit from more precise patient positioning and breath control systems.

**Table 1:** Patient characteristics. Values are given for the smallest margins sufficient for total dose V95>95%

Patient	Fields	Baseline (week 1)		Follow-up (week 2-6)		Difference ITV – 4D		
		Amplitude [mm]	Volume [cc]	Amplitude (Range) [mm]	Margins V95>95%	D5-D95 [%]	CI [%]	Lung V20 [%]
P1	3	3.3	236.5	2.8 - 3.9	3 + 2	2.4	14.4	1.2
P2	3	12.6	160.2	6.6 - 15.9	7 + 2	5.1	28.3	1.4
P3	2	5.6	44.7	2.1 - 5.4	3	-1.5	90.0	0.5
P4	3	22.2	125.3	20.6 - 27.5	5 + 3	0.8	5.8	1.1

## 2) Pencil beam scanning proton therapy of lung cancer: Impact of interplay effect

Annika Jakobi<sup>1</sup>, Antje Knopf<sup>2,3</sup>, Rosalind Perrin<sup>2</sup>, Christian Richter<sup>1</sup>

<sup>1</sup>OncoRay - National Center for Radiation Research in Oncology, High Precision Radiotherapy Group, Faculty of Medicine and University Hospital Carl Gustav Carus, TU Dresden, Helmholtz-Zentrum Dresden-Rossendorf, Dresden, Germany, <sup>2</sup>Paul Scherrer Institute, Center for Proton Therapy, Villigen, Switzerland, <sup>3</sup>now with: Joint Department of Physics at The Institute of Cancer Research and The Royal Marsden NHS Foundation Trust, London, UK

For a patient cohort of 40 patients with small tumour volumes, the impact of tumour motion in active scanned proton therapy was evaluated based on machine parameters of the proton therapy at the University Hospital Dresden. For two patients the changes in the prospectively estimated 4D dose distribution was recalculated for a sequential 4D-CT data set. Furthermore, for subgroups of 9-10 patients, the influence of treatment planning concepts (e.g. target concept, single field versus multi field optimization), parameter variations (e.g. variations of energy layer switching time and breathing pattern) and motion mitigation (gating, rescanning) was assessed.

4D dose distributions of the patient cohort showed relevant dose degradation mainly for patients with cranio-caudal motion amplitudes above 5 mm (Figure 1). Single fraction dose degradation reduced dose coverage in terms of  $V_{95}$  by median 13% with maximum of 59%. High dose volumes in terms of  $V_{107}$  were increased by median 8% with up to 52%. For none of the patients the dose in the target was degraded to below 80% of the prescribed dose and rarely increased above 120%. Dose parameters for organs at risk were not changed compared to the static case for most patients. Fractionation reduced the dose degradation due to averaging effects.

The assessment of the 4D dose distribution on a sequential 4D CT for two patients revealed the impact of changed patient anatomy: for one patient a relevant change of the motion occurred (increase of 5 mm of the cranio-caudal motion amplitude) accompanied by a baseline shift. Dose coverage for this patient was largely hampered compared to the original 4D dose distribution. The second patient showed only minor anatomical changes. The expected 4D dose distribution remained rather unchanged compared to the prospectively estimated one.

We showed that dose degradation was mainly relevant for patients with motion amplitudes above 5 mm. Prospective estimations of dose degradation might support treatment decisions. However, changes in patient anatomy might hamper the reliability of such estimations and should be included in treatment evaluations during treatment. The assessment of the dosimetric impact of anatomical changes might support decisions for treatment plan adaptation.

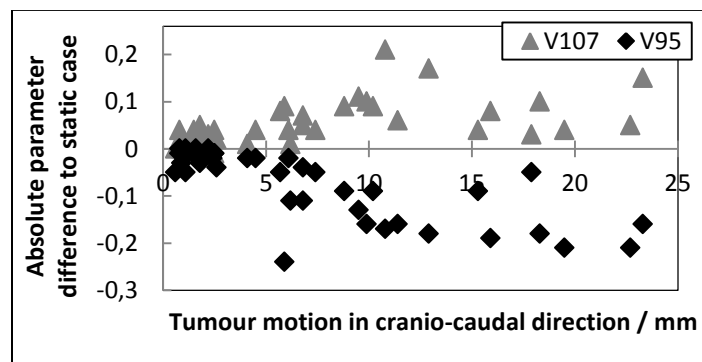


Figure 1: Difference between the median 4D dose parameter and the static case for  $V_{95}$  and  $V_{107}$  for a single fraction.

### 3) Quantification of interplay effects of PBS-based lung tumour treatments under various fractionation schemes with/without rescanning: the Varian ProBeam experiences

Ye Zhang<sup>1,2</sup>, Isabel Huth<sup>2</sup>, Martin Wegner<sup>2</sup>, Damian Weber<sup>1</sup>, Tony Lomax<sup>1</sup>

<sup>1</sup>Center for Proton Therapy, Paul Scherrer Institut, Villigen-PSI, Switzerland, <sup>2</sup>Varian Medical Systems – Particle Therapy GmbH, Troisdorf, Germany

This study aims to investigate how much fractionation treatment can influence the impact of interplay and whether rescanning is still necessary for achieving an acceptable target dose distribution.

For an example lung tumour case (CTV volume of 18.8cc and motion of 12mm), three-field 3D plans (AP, LR, and 45 degree) were calculated on both a patient specific geometric ITV (gITV) and range-adapted ITV (rITV) using a spot spacing of 4mm orthogonal to the beam directions. 4D dose calculations were performed, simulating three different fractionation treatments with schemes of 2.5 Gy x 35fx (A), 5 Gy x 10fx (B) and 13.5 Gy x 3fx (C), based on machine and delivery parameters of the Varian ProBeam system (lateral scanning speed of 5/20 mm/ms and energy switching time of 700 ms with layer-wise optimized dose rates). 1x- to 19x-layered and volumetric rescanning was simulated to mitigate residual motion effects. The final dose distributions were obtained by superposition and normalization of the 4D dose distributions of each field and each fraction with random starting phases of the 4DCT (10 different phases with 100 random starts). We use the dose to 99% of the target (D99) and homogeneity index (HI:D5-D95) in CTV as metrics to quantify the resultant 4D dose distributions within the target, while for the normal lung (both lungs minus CTV), V20 and mean lung dose (MLD) were also compared.

For single fraction (of the whole fractionation) scenarios, the normalized interplay magnitudes are similar among the different schemes. The absolute D5-D95 value (gITV plans) is  $0.3 \pm 0.09$ ,  $0.6 \pm 0.17$  and  $1.6 \pm 0.45$  Gy higher than the static value for the schemes A, B and C respectively. In comparison to the single fraction, for the conventional scheme A, the normalized D5-D95 is lower than the static value. For hypo-fractionation scheme B, the mean HI is equal to the static value with  $\pm 1\%$  variations due to the presence of the random starting phases. For hypo-fractionation scheme C, HI becomes  $2.5 \pm 2.5\%$  higher than the static case. However, all schemes were able to achieve a comparable dose distribution to the static reference, once combined with moderate rescanning ( $< 5x$ ). In addition, the variabilities (e.g. as a function of starting phase) have been reduced to within 1%, independent of the rescanning technique used, but a few more rescans are needed for hypo-fractionation schemes than for conventional scheme. Moreover, the hypo-fractionated plans provide a significantly reduced normal lung exposure, with MLD and V20 reducing to 22 Gy and 8% compared to 45 Gy and 12% for the conventional scheme. In addition, 4D rITV plans have better dose converge and homogeneity (5% w.r.t static) than corresponding gITV plans, with a cost of slightly worse MLD (2.2 Gy) and V20 (0.5%) (max. value for all schemes) to the normal lung.

In conclusion, fractionation can lead to an improved target dose distribution and significantly spared normal lung exposure. The starting phase induced variability is only obvious when a large fraction dose is used and can be reduced once rescanning is applied.

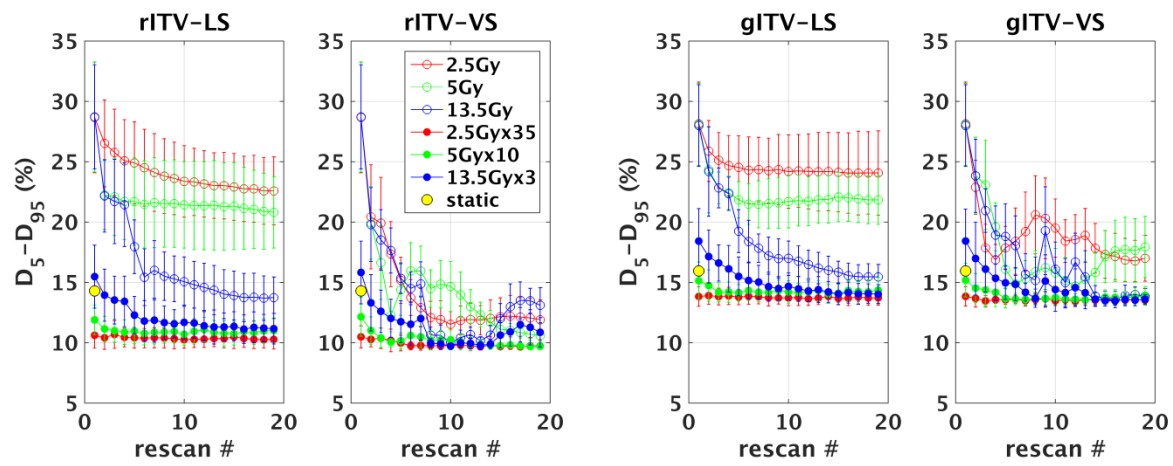


**Figure 1:**  $D_5 - D_{95}$  (CTV) with a function of rescan number for 4D plans calculated on (left) rITV and (right) gITV using layered (LS) and volumetric (VS) rescanning with different fractionation schemes.

#### 4) Limited impact of breathing motion, interplay effect and set-up/range uncertainties in IMPT for advanced stage NSCLC

Tatsuya Inoue<sup>1</sup>, Lisanne V. van Dijk<sup>2</sup>, Joachim Widder<sup>2</sup>, Hideki Takegawa<sup>3</sup>, Masahiko Koizumi<sup>4</sup>, Masaaki Takashina<sup>4</sup>, Anneyuko I. Saito<sup>1,5</sup>, Keisuke Sasai<sup>5</sup>, Aart A. van't Veld<sup>2</sup>, Johannes A. Langendijk<sup>2</sup>, Erik W. Korevaar<sup>2</sup>

<sup>1</sup>Department of Radiology, Juntendo University Urayasu Hospital, Japan, <sup>2</sup>Department of Radiation Oncology, University of Groningen, University Medical Center Groningen, The Netherlands, <sup>3</sup>Department of Radiology, Kansai Medical University, Japan, <sup>4</sup>Department of Medical Physics and Engineering, Osaka University Graduate School of Medicine, Japan, <sup>5</sup>Department of Radiation Oncology, Juntendo University Graduate School of Medicine, Japan

**Purpose:** To investigate the impact of breathing motion, interplay effect with scanning beams, and set-up/range uncertainties employing 4D dose accumulation in robustly optimized intensity modulated proton therapy (IMPT) for advanced stage non-small cell lung cancer (stage III NSCLC).

**Materials and methods:** Three-field IMPT treatment planning was performed with RayStation for 10 stage III NSCLC patients that had been treated with the partial VMAT planned in Pinnacle. Minimax robust optimization accounted for 5 mm or 7 mm systematic set-up errors and 3% range uncertainty to deliver 60 Gy to CTV in 25 fractions. Plans were recalculated on eight 4D-CT phases and accumulated after deforming the dose of each phase onto a reference CT, which corresponded to the phase of maximal expiration. Dose distributions including 1) breathing motion, 2) interplay effect and 3) isotropic 5 mm set-up error and  $\pm 3\%$  range uncertainties (total 54 scenarios) for each patient as well as the combination of 1) and 3) (total 80 scenarios) were obtained using in-house programming. Homogeneity index (HI: D2-D98) and target coverage (TC: V95%) for CTV and dose statistics for lung, esophagus, heart and spinal cord were evaluated and compared to the clinical photon plans.

**Results:** HI and TC in each patient were within clinical limits taking into account breathing motion and similarly interplay effect if rescanning (or fractionation) was assumed. The set-up/range uncertainties had a larger impact and with both set-up/range uncertainties and breathing motion included, TC decreased to below 98% in 3 out of 10 patients for the 5 mm robust plans. This was solved in the 7 mm robust plans. OAR dose values did not vary significantly for three types of errors. The 7 mm robust plans had slightly higher OAR doses than the 5 mm plans, e.g. the mean lung dose increased by 0.3 Gy. Compared to the nominal photon plans, the proton plans showed better target homogeneity, reduced the mean lung dose about 40% and reduced the mean heart dose about 60%.

**Conclusions:** Robustly optimized IMPT plans and rescanning/fractionation resulted in robustness against breathing motion, interplay effect and set-up/range uncertainties for advanced stage NSCLC patients. Set-up/range uncertainties showed the largest impact on target coverage and increasing the parameter that takes into account set-up error in the robust optimization could compensate for the impact of breathing motion, interplay effect and set-up/range uncertainties. Robustly optimized IMPT also had comparable or improved target dose homogeneity and can significantly reduce the lung and heart doses compared to the photon plans.

**Acknowledgement:** This study was supported by Japan Society for the Promotion of Science (JSPS) Core-to-Core program (No. 23003).

## 5) Planning studies for non-invasive treatment of cardiac arrhythmias with scanned carbon ion beams

Anna Constantinescu, PhD<sup>1</sup>; H. Immo Lehmann, MD<sup>2</sup>; Christoph Bert, PhD<sup>1,3</sup>; Douglas L. Packer, MD<sup>2</sup>; Marco Durante, PhD<sup>1</sup>; and Christian Graeff, PhD<sup>1</sup>

<sup>1</sup>GSI Helmholtz centre, Darmstadt, Germany, <sup>2</sup>Mayo Clinic College of Medicine, Rochester, MN 55905, USA, <sup>3</sup>University Clinic Erlangen, Erlangen, Germany

Cardiac arrhythmias are a major, worldwide health burden. Catheter ablation is the current gold standard treatment. Through scar formation, unwanted signals are isolated or interrupted, e.g. from the pulmonary veins (PV), the atrioventricular node (AVN) or in the left ventricular wall (LV). The feasibility to induce electrophysiological changes non-invasively with <sup>12</sup>C has been successfully demonstrated by our group in an animal model. We present treatment planning studies in human data for the common ablation regions.

Heartbeat-gated 4DCTs of 5 patients were acquired. Targets for ablation of PV, AVN and LV as well as OARs were contoured. Treatment planning studies were carried out with the in-house treatment planning software TRiP4D. Treatment fields were optimized either individually (SFUD) for AV and LV or together (IMPT) for PV due to the nearby esophagus. Physical target doses of 40 Gy, 55 Gy (SFUD) and 25 Gy, 40 Gy (IMPT) were simulated in a single fraction. Rescanning and gating were used as motion mitigation techniques. Dose deposition in OARs (heart, aorta, trachea, esophagus) were compared to literature values for single fraction X-ray deliveries (dose-volume limits for aorta: 31 Gy to 10 cc, heart: 16 Gy to 15 cc, esophagus: 11.9 Gy to 5 cc, trachea: 10.5 Gy to 4 cc).

AVN displacement had a mean motion in-between the most extreme motion phases of  $10.5 \pm 1.3$  mm. Displacement of LV and PVs had similar maximal amplitudes, with a mean displacement of less than 5 mm. Irradiations with at least 10 rescans were sufficient to yield homogenous target coverage in case of AVN and PV irradiations. For the irradiation of LV with two non-opposing fields, rescanning within a 55% gating window was necessary. The dose-volume depositions to aorta and trachea were non-critical for all studied cases. In case of PV target volumes, the dose to the esophagus resulted to be exceeded in some of the patient cases for a 40 Gy delivery.

Treatment planning with scanned carbon ions for the non-invasive ablation of cardiac target volumes was carried out. A delivery approach to overcome the influence of cardiac motion was developed and the resulting dose deposition in the OARs was studied. Scanned carbon ion beams have the potential to become an accurate, less operator-dependent, fast and catheter-free treatment approach for cardiac arrhythmias.

## 6) Changing from ITV to MidV concept – Do we have to adapt the prescribed dose?

S. Ehrbar<sup>1,2</sup>, A. Tartas<sup>1,3</sup>, L. S. Stark<sup>1,2</sup>, S. Klöck<sup>1,2</sup>, M. Guckenberger<sup>1,2</sup>, S. Lang<sup>1,2</sup>

<sup>1</sup>University Hospital Zurich, Department of Radiation Oncology, Zürich, Switzerland, <sup>2</sup>University of Zurich, Faculty of Science, Zurich, Switzerland, <sup>3</sup>University of Warsaw, Faculty of Physics, Warsaw, Poland

**Introduction:** The internal target volume (ITV) concept is a commonly used concept for stereotactic body radiation therapy (SBRT) of lung cancer. Recently, the mid-ventilation (MidV) principle which is a probabilistic margin approach was introduced. This approach leads to a reduction of the margin and a better sparing of healthy tissue. We investigated, whether the prescribed dose needs to be adapted, changing from the ITV to the MidV concept to ensure tumor dose coverage.

**Materials and Methods:** Nineteen lung cancer patients with internal tumor motion from 5 to 27 mm were analyzed in this study. For all patients four-dimensional (4D) CT scans were used for generation of treatment plans for ITV and MidV concepts. The full tumor excursion was delineated as ITV and planning target volume (PTV) margins of 5 mm were added. For the MidV concept, margins according to the van-Herk formula were added to the gross tumor volume (GTV) in the MidV respiration phase. VMAT treatments plans (3D dose) were calculated with a 3x13.5 Gy dose prescription (D95) to the 65% isodose line around the PTV for both techniques. Timeresolved 4D dose calculations, linking breathing motion and dynamic delivery, were performed. The dynamic dose to the GTV was summed up in MIM Maestro (MIM Software Inc., USA) using deformable image registrations between the respiratory phases of the 4DCT. The summed up 4D doses to the GTV using ITV and MidV concepts were compared.

**Results:** The 3D dose calculations yielded an ITV (resp. GTV for MidV plans) mean dose of 60.2 ( $\pm 0.4$ ) Gy (mean  $\pm$  std). The 3D mean dose to the lung volume was decreased by 19% ( $\pm 8\%$ ) for the MidV concept compared to ITV concept. The time resolved 4D dose calculations lead to an increase in GTV mean dose for the ITV concept to 60.7 ( $\pm 0.5$ ) Gy and a decrease in GTV mean dose for the MidV concept to 58.3 ( $\pm 0.8$ ) Gy. Over all, the dynamic GTV mean dose was decreased by 4.0% ( $\pm 1.3\%$ ) when changing from the ITV to the MidV concept.

**Conclusion:** It is recommended to increase the dose per fraction from 13.5 Gy to 14 Gy when changing from the ITV concept to the MidV concept in order to ensure an equivalent GTV dose coverage. The change in treatment concept including the increased fraction dose leads to a reduced mean lung dose by 16%.

## 7) A strategy for robust radiotherapy treatment plans for pre-operative oesophageal cancer

S Warren, M Partridge, S Mukherjee, MA Hawkins

CRUK/MRC Oxford Centre for Radiation Oncology, University of Oxford, Oxford OX3 7DQ. UK

**Aim:** To determine a method for creating robust photon and proton plans for pre-operative oesophageal cancer patients using 4D-CT datasets, with a view to reduce post-operative complications, such as cardio-pulmonary toxicity and anastomosis.

**Method/Materials:** Radiotherapy treatment plans using photons and protons have been optimised on a 4D CT dataset for a representative patient (diaphragm motion of 1.6 cm during breathing). The reference plan (50.4 Gy / 28 fractions) optimised on the average phase of the 4D-CT (4D\_Ave) was re-calculated on each phase of the 4D-CT, and using deformable image registration this 'free-breathing' dose was accumulated and displayed on the original 4D\_Ave dataset for comparison. The possible benefits of respiratory gating for sparing normal tissue (assuming a 30% duty cycle around end exhale) were examined. Set-up errors of  $\pm 5$  mm (and range errors of  $\pm 3.5\%$  for proton plans) were also simulated. Coverage of the target volume, as well as dose-metrics for heart, lung and stomach were recorded.

**Results:** For the representative patient, photon and proton reference plan dose was almost identical to the dose accumulated across all phases of the 4D-CT (Table), and the proton plan showed superior normal tissue sparing.

	Proton		Photon	
	Reference (Gy)	Accumulated (Gy)	Reference (Gy)	Accumulated (Gy)
CTV D <sub>98</sub>	50.5	50.6	50.6	49.7
Heart mean	7.6	7.7	16.0	15.8
Lung mean	3.5	3.5	7.8	7.8
Stomach D <sub>50</sub>	33.4	33.1	33.7	33.4

Respiratory gating improved heart sparing for photons (reduction of mean dose to 12.1 Gy) but the reduction in mean heart dose was only 1 Gy for the proton plan.

The analysis of perturbed plans with set-up and range uncertainties show robust target coverage for both techniques: CTV D98 minimum = 49.6 Gy (proton) and 48.7 Gy (photon). However, median stomach dose shows greater variation in the perturbed plans for protons (D50 range 15.5 to 42.5 Gy) than photons (D50 range 31.8 to 35.3 Gy).

**Conclusions:** A method to optimise dose distributions which are robust to intra-fraction breathing motion has been demonstrated on a representative patient. This method works for both photon and proton plans and is sufficiently robust to set-up and range error. Further testing on patients with larger breathing amplitude and with variable stomach and bowel filling during treatment is underway.

## 8) Validation of a tool for monitoring inter-fractional anatomical changes in abdominal patients

V. Batista<sup>1</sup>, W. Chen<sup>2</sup>, Z. Asim<sup>1,4</sup>, J. Bauer<sup>1,2</sup>, K. Parodi<sup>2,5</sup>, K. Herfarth<sup>1</sup>, J. Debus<sup>1</sup>, O. Jäkel<sup>2,3</sup>

<sup>1</sup>University Clinic of Heidelberg, Germany; <sup>2</sup>Heidelberg Ion-Beam Therapy Center (HIT), Heidelberg, Germany, <sup>3</sup>German Cancer Research Center (DKFZ), Heidelberg, Germany, <sup>4</sup>Lisbon School of Health Technology, Lisbon, Portugal, <sup>5</sup>Ludwig-Maximilians-University, Munich, Germany

**Purpose and Background:** Heavy-ion radiotherapy enables a conformal irradiation of the tumour with minor dose deposition in the healthy tissue. However, its high sensitivity to inter-fractional anatomical changes strongly affects the treatment quality. Complexity and time consumption limit the plan adaptation. Therefore, we suggest a method to estimate anatomical changes, based on water-equivalent path length (WEPL) variations, and correlate them with dosimetric indicators to assess the need of replanning.

**Materials and Methods:** Two pancreatic and two hepatocellular carcinoma patients were selected in order to validate a MeVisLab<sub>[1]</sub>-module computing the WEPL in follow-up CT-images, acquired on a regular basis. For each patient, the accumulated-WEPLs (accWEPL) in the beam-path were compared between the planning-CT and each of the pre-treatment-CTs. To increase the set of possible WEPL variations, new plans were optimized for different beam geometries, and forward-calculated in each CT. The dose forward-calculation was performed using the research planning system TRiP98<sub>[2]</sub>. V95 and the homogeneity index were used as metric of the dose distribution, while for the accWEPL-maps the mean variation and fraction of voxels with more than 3 mm- $\Delta$ WEPL were used. Additionally, the gamma-index<sub>[3]</sub> was calculated for the dose and accWEPL distributions, as common indicator of geometric and dosimetric variations.

**Results:** Variations larger than 5% in the V95<sub>CTV</sub> resulted in detectable variation of the accWEPL in terms of an increased fraction of voxels exceeding a 3mm variation ( $\geq 40\%$ ). Gamma-index maps from dose distributions and accWEPL maps showed to be similar, which supports the soundness of this method. Figure 1 reports an example of the performed analysis.

**Conclusions/Outlook:** The evaluated method has proven to be a valuable tool to predict the impact of inter-fractional anatomic variations on the dose distribution, with low computation time and no contouring. This analysis will be extended to a larger patient-cohort and used to support the definition of thresholds and further improvement of the clinical protocols.

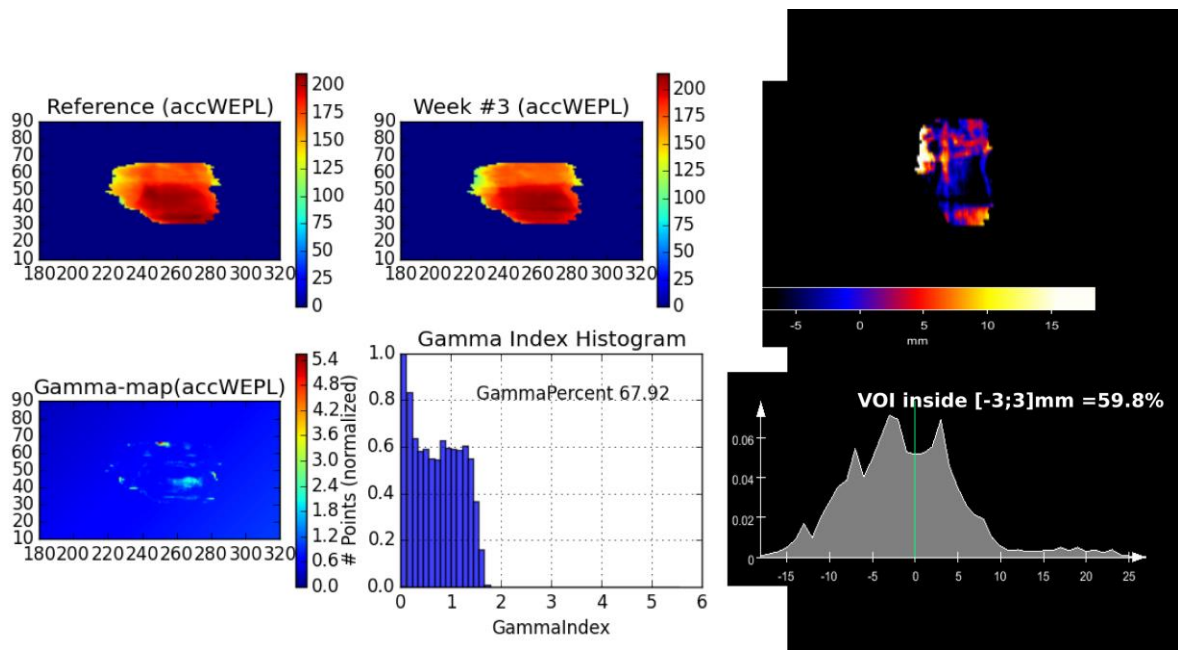


**Figure 1:** Analysis of accWEPL-variations between the planning CT (a), the 3rd week follow-up CT (b), and the difference-map(c). In the lower row is shown the Gamma-map (d) and -histogram of the accWEPL (e) and the histogram (f) of the  $\Delta$ accWEPL from c). This case corresponds to a simulation of a pancreatic patient with a single lateral beam, exhibiting a dose reduction in the V95CTV of 8%.

#### References

- [1] Unholtz D, et al. Conference Record of IEEE 2011 NSS-MIC.
- [2] Krämer M, et al. Phys. Med. Biol., 45/11, 2000, 3299 – 3317
- [3] Spezi E, et al. Radiotherapy and Oncology 79 (2006) 224–230

## 9) Influence of organ motion on relative risks of radiation-induced secondary cancer for VMAT and IMPT of prostate cancer

Stokkevåg CH<sup>1,2</sup>, Engeseth GM<sup>1</sup>, Hysing LB<sup>1</sup>, Ytre-Hauge KS<sup>2</sup>, Muren LP<sup>3</sup>

<sup>1</sup>Department of Oncology and Medical Physics, Haukeland University Hospital, Bergen, Norway, <sup>2</sup>Department of Physics and Technology, University of Bergen, Bergen, Norway, <sup>3</sup>Department of Medical Physics, Aarhus University / Aarhus University Hospital, Aarhus, Denmark

**Background and aim:** An elevated risk of radiation-induced secondary cancer (SC), particularly in directly irradiated tissues such as the bladder and rectum, has been observed in prostate cancer patients after radiotherapy (RT). There are considerable fluctuations in SC risk due to inter-patient anatomy variations, indicating the relevance of also including the effects of variations in organ position and shape for individual patients. Both the bladder and rectum are highly mobile structures and the aim of this study was therefore to investigate the influence of organ motion on SC risk.

**Methods and Materials:** Simultaneously integrated boost treatment plans were generated for ten prostate patients using volumetric modulated arc therapy (VMAT) and intensity-modulated proton therapy (IMPT). Both VMAT and IMPT plans were prescribed to deliver 67.5 Gy to the prostate and 60 Gy to the seminal vesicles over 25 fractions, using fiducial marker based image guidance. Each patient had 8-9 repeat CT scans throughout the course of treatment on which the bladder and rectum were re-contoured. For three of the patients the doses were recalculated on the repeat scans using the originally planned dose distributions. The dosimetric and volumetric distributions for each treatment plan were evaluated with respect to relative risk of radiation-induced cancer by using the organ equivalent dose concept adapted to dose-response models reflecting varying degrees of cell sterilisation: a linear model, a linear-plateau model and a bell-shaped model.

**Results:** The choice of model as well as each dose distribution contributes to SC risk fluctuating in favour of either IMPT or VMAT. Similar variations were seen across repeat CT scans for two of the patients, while for the third patient the SC risk estimates were consistently lower for IMPT across all models and repeated CT scans.

**Conclusions:** Day-to-day variations in anatomy lead to fluctuations in SC risk estimates that are of the same magnitude as the inter-patient variations.

## 10) Investigation of magnetic field and motion effects on IMRT dose delivery using Monte Carlo simulations

O. Schrenk<sup>1</sup>, C. K. Spindeldreier<sup>1</sup>, O. Jäkel<sup>1,2</sup>, A. Pfaffenberger<sup>1</sup>

<sup>1</sup>German Cancer Research Center (DKFZ), Im Neuenheimer Feld 280, Heidelberg, <sup>2</sup>Heidelberg Ion-Beam Therapy Center, Im Neuenheimer Feld 450, Heidelberg

Novel hybrid devices combining the advantages of MR imaging and radiation treatment have the potential to increase the accuracy of radiation therapy. It is known that the magnetic field of the MR manipulates the trajectory of the secondary electrons and leads to a change of dose especially at the interfaces between materials of high and low densities [Raaijmakers2005]. In this work, the interaction of the altered dose distribution and intrafractional motion for the therapy of lung cancer with a MRILINAC machine is investigated.

An EGSnrc Monte Carlo [Kawrakow2013] environment was developed which allows the simulation of dose delivery of IMRT treatment plans to patient CT data in the presence of a magnetic field. A routine for the processing of treatment planning parameters and Monte Carlo simulation results was implemented into the in-house open source treatment planning system matRad. In order to validate the routine dose distributions were compared against collapsed cone calculations by the treatment planning system Raystation and to dosimetric gel measurements in an anatomical porcine lung phantom [Remmert2007], without the presence of a magnetic field. Results show that the Monte Carlo simulations are in good agreement to the Raystation results and the agreement of gel measurements is within 5% in the center of the planning target volume. First investigations of the effect of a 1.5 T lateral magnetic field to the dose distribution in a simple lung tumor case, compared to the same IMRT plan applied without a magnetic field, show only slight differences of tumor dose but evident dose enhancements in lung tissue and skin (see Figure 1).

In the next step, the routine will be modified to perform Monte Carlo simulations in time resolved CT data. This will allow the identification of the impacts caused by anatomical changes during respiration and provide the possibility to investigate optimization strategies for lung treatment planning with a MRILINAC system.

**Acknowledgments:** We thank Dr. Iwan Kawrakow for providing the magnetic field macro for the EGSnrc code system and Philipp Mann for providing the measurement in the porcine phantom.

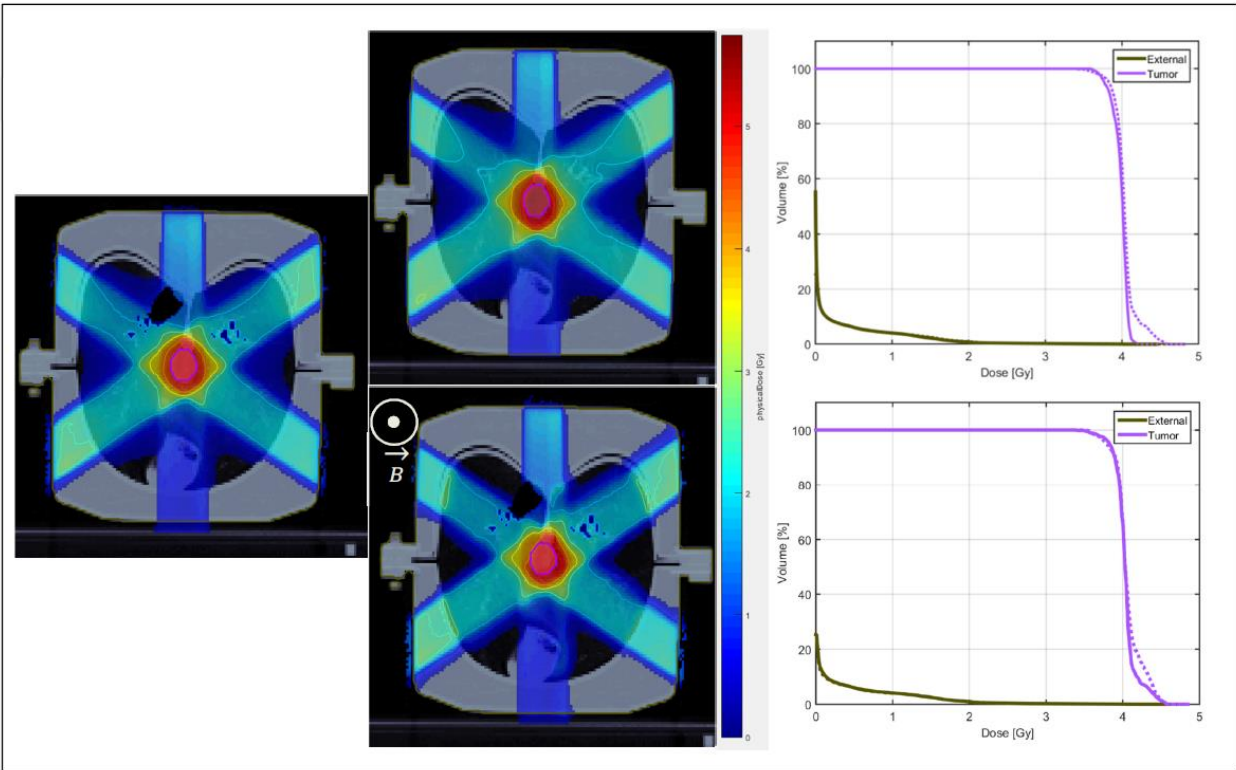


**Figure 1:** Left: Dose distribution derived from Monte Carlo simulation without the presence of a magnetic field. Middle top: Dose distribution calculated with the Raystation treatment planning system. Middle bottom: Dose distribution in the presence of a lateral 1.5 T magnetic field. Right Top: Dose-volume histogram for the Raystation dose distribution (solid lines) and 0 T (dashed lines) Monte Carlo simulation. Right bottom: Dose-volume histogram for 0 T (solid lines) and 1.5 T (dashed lines) simulations.

### 11) Initial clinical experience of spot-scanning proton beam therapy using real-time-image gated proton-beam therapy system

Shinichi Shimizu<sup>1,2</sup>, Norio Katoh<sup>2,3</sup>, Kentaro Nishioka<sup>1</sup>, Takayuki Hashimoto<sup>4</sup>, Tetsuya Inoue<sup>3</sup>, Taeko Matsuura<sup>5</sup>, Seishin Takao<sup>6</sup>, Yuka Matsuzaki<sup>6</sup>, Yusuke Fujii<sup>6</sup>, Masaya Tamura<sup>6</sup>, Rikiya Onimaru<sup>4</sup>, Kikuo Umegaki<sup>5</sup>, Hiroki Shirato<sup>1,2</sup>

<sup>1</sup>Department of Radiation Oncology, Hokkaido University Graduate School of Medicine, Sapporo, Japan, <sup>2</sup>Global Station for Quantum Medical Science and Engineering, Global Institution for Collaborative Research and Education (GI-CoRE), Hokkaido University, Sapporo, Japan, <sup>3</sup>Department of Radiation Oncology, Hokkaido University Hospital, <sup>4</sup>Department of Radiation Medicine, Hokkaido University Graduate School of Medicine, Sapporo, Japan, <sup>5</sup>Faculty of Engineering, Hokkaido University, Hokkaido University, Sapporo, Japan, <sup>6</sup>Department of Medical Physics, Hokkaido University Graduate School of Medicine / School of Medicine, Sapporo, Japan

**Background/Purpose:** We have developed a spot-scanning proton beam therapy (SSPT) system gated with the use of a real-time tumor-tracking function through two sets of fluoroscopic X-ray in the gantry and fiducial markers inserted around the target, which we call real-time-image gated proton beam therapy (RGPT). The SSPT for static tumors has been in operation since March 2014 and RGPT for moving tumors since December 2014. The characteristics of the enrolled patients and the monitoring reports about them are reported as the initial clinical experience.

**Materials/Methods:** Fifty-six patients, 41 male and 15 female, with 59 lesions enrolled on a prospective clinical trial to evaluate the clinical outcome of radiation therapy using SSPT from March 2014 to June 2015. In the 56 patients, 20 patients with 22 lesions were treated using the RGPT system. Patients were seen every week during SSPT, every month for the first 3 months after SSPT and every 3 months thereafter. Adverse events were recorded and assessed according to CTCAE version 4.03.

**Results:** The median age was 66 years old (range 1-87). The median radiation dose of 60 GyE (RBE=1.1) (range 20-76) was administered in 26 fractions (range 4-35) to 99% of the clinical target volume. Treatment sites were as follows: 16 prostate, 12 liver, 7 bone and soft tissue, 5 lung, 5 central nerve system and 14 others. Of the 22 lesions treated using the RGPT system, 11, 2, and 9 were liver, lung, and prostate. All patients completed SSPT except for one patient whose treatment was interrupted due to out-field disease progression. No patient experienced treatment interruption due to adverse events. 7 patients experienced grade 3 or more adverse events with the median follow-up time of 244 days (range 86 - 450). Among 20 patients treated using the RGPT system, no patients experienced grade 3 or more adverse events during the course of treatment and follow up period.

**Conclusion:** Our data showed that SSPT using RGPT is feasible without serious adverse effects for initially enrolled patients with liver, lung, and prostate cancers. Prospective study is required to investigate its efficacy comparing to standard treatment.

## 12) Efficacy assessment of abdominal compression in 4DCT

Andrea Pella<sup>1</sup>, Piero Fossati<sup>1,2</sup>, Silvia Molinelli<sup>1</sup>, Matteo Seregini<sup>3</sup>, Riccardo Via<sup>3</sup>, Marco Riboldi<sup>3</sup>, Francesca Valvo<sup>1</sup>, Mario Ciocca<sup>1</sup>, Sandro Rossi<sup>1</sup>, Roberto Orecchia<sup>1,2,4</sup>, Guido Baroni<sup>1,3</sup>

<sup>1</sup>CNAO Foundation, Clinical Division, Pavia, Italy, <sup>2</sup>University of Milan, Milano, Italy, <sup>3</sup>Politecnico di Milano, Department of Electronics Information and Bioengineering, Milano, Italy, <sup>4</sup>European Institute of Oncology, Division of Radiotherapy, Milano, Italy

In external beam radiotherapy the need of time-resolved tumor targeting methodologies arises in presence of not negligible organ motion. Four-dimensional CT (4DCT) is commonly used to image anatomy variations as a function of patient breathing. Gated irradiation represents a possible solution to minimize the effects of target (and/or organ at risks) motion using a surrogate signal representative of breathing dynamics. At CNAO, a gating protocol for carbon ion therapy has been developed. It combines also abdominal compression (through tight thermoplastic body masks) and active beam rescanning. Treatment is optimized using the end-exhale (EE) phase and it is delivered in a gate-on window centered on the same phase. Anzai system (Anzai Medical CO., LTD) is used for both 4DCT-based treatment planning and delivery.

The aim of this study is to investigate the efficacy of motion mitigation tools in reducing target excursion during breathing. We report the 3D GTV displacements observed between end-exhale and end-inhale (EI) phases of the planning 4DCT.

At this time, data of eleven patients with thoracic and abdominal lesions has been evaluated. A B-spline-based deformable registration algorithm (Plastimatch) was used to calculate the displacement field between EE and EI volumes. GTV contours, as segmented by medical doctors in EE phase, were then propagated to the EI phase.

A median (interquartile) 3D displacement of 4.55 (2.06) [mm], in a range of 0.48-10.09 [mm] was found. The maximum displacements (absolute values) were noticed in superior/inferior direction (range: 0.21-8.89 [mm]).

Such displacements can be considered relevantly lower than those reported in literature for abdominal lesions, where ranges of motions consistently larger than 10 mm were observed. Furthermore, irregularities in a patient's respiratory pattern (and thus in target trajectory) can often be reduced by means of appropriate immobilization/compression tools. This approach consequently tends to reduce the overall tumor localization uncertainty during irradiation.

### **13) Respiratory gating guided by internal electromagnetic motion monitoring during stereotactic radiation therapy in the liver**

P R Poulsen, E S Worm, R Hansen, J B B Petersen, L P Larsen, C Grau, and M Høyer

*Aarhus University Hospital, Aarhus, Denmark. per.poulsen@rm.dk*

**Aim** Intra-fraction motion may compromise the target dose of SBRT treatments of tumours in the liver. Respiratory gating can improve the treatment delivery, but gating based on external surrogates may be inaccurate. This study investigates the accuracy of gated liver SBRT treatments guided by internal motion monitoring by implanted electromagnetic transponders.

**Method** Four patients with solitary liver metastases were treated in three fractions with respiratory gated SBRT guided by three implanted electromagnetic transponders. The treatment was delivered in end-exhale with beam-on when the centroid of the three transponders deviated less than 3 mm (LR and AP directions) and 4 mm (CC) from the planned position. Log files were used to determine the transponder motion during beam-on in the actual gated treatments and in simulated non-gated treatments with CBCT setup. The motion was used to reconstruct the delivered CTV dose distribution with and without gating. The reduction in  $D_{95}$  (minimum dose to 95% of the CTV) relative to the plan was calculated for each treatment fraction of the two first patients.

**Results** With gating the maximum course mean geometrical error in any direction was 1.2 mm. Without gating systematic baseline drifts during the treatment session resulted in course mean errors ranging from -2.8 mm to 1.2 mm (LR), from 0.74 mm to 7.1 mm (CC), and from -2.6 mm to 0.1 mm (AP). The reduction in CTV  $D_{95}$  was 0.5% (gating) and 12.1% (non-gating) for Patient 1 and 0.3% (gating) and 1.7% (non-gating) for Patient 2. The mean duty cycle was 59% (range 54-70%).

**Conclusion** Respiratory gating based on internal electromagnetic motion monitoring was performed for four liver SBRT patients. The gating added robustness to the dose delivery and ensured a high CTV dose even in the presence of large intra-fraction motion.

#### **14) Treatment of liver tumors close to the skin surface with real-time image gated, spot-scanning proton beam therapy (RGPT) system – comparison between range compensation devices**

Taeko Matsuura<sup>1,2,3</sup>, Seishin Takao<sup>1</sup>, Yuka Matsuzaki<sup>1</sup>, Yusuke Fujii<sup>1</sup>, Takaaki Fujii<sup>1</sup>, Naoki Miyamoto<sup>1</sup>, Norio Katoh<sup>4</sup>, Shinichi Shimizu<sup>1,2,4</sup>, Hiroki Shirato<sup>1,2,4</sup>, Kikuo Umegaki<sup>1,2,3</sup>

<sup>1</sup>Proton Beam Therapy Center, Hokkaido University Hospital, North-15 West-7, Kita-ku, Sapporo, Hokkaido, 060-8638, Japan, <sup>2</sup>Global Station for Quantum Medical Science and Engineering, Global Institution for Collaborative Research and Education (GI-CoRE), Hokkaido University, Sapporo 060-8648, Japan, <sup>3</sup>Faculty of Engineering, Hokkaido University, North-13 West-8, Kita-ku, Sapporo, Hokkaido, 060-8628, Japan, <sup>4</sup>Department of Radiation Oncology, Graduate School of Medicine, North-15 West-7, Kita-ku, Sapporo, Hokkaido, 060-8638, Japan

It has been a challenging issue to apply a spot-scanning proton therapy to respiratory-moving tumors due to the possibility that the interplay between tumors and narrow scanning beams makes hot and cold spots in tumors. We use a real-time gating system in clinical practice which suppresses the deviation of actual spot position from the planned position to within 2 mm and makes it possible to deliver dose to patients with high accuracy (Shimizu *et al.*, PLOS ONE (2014)).

Here we considered the methods using the gating system for treating liver tumors, part of which is located at depth less than 4 g/cm<sup>2</sup>. The commercial spot-scanning systems available cannot generate the low-energy beams whose range is less than 4 g/cm<sup>2</sup>, which necessitates a range compensation device to be placed below the nozzle. We considered the following three options: (i) a mini ridge-filter combined with a range shifter (Matsuura *et al.*, AAPM2015), (ii) a range shifter, and (iii) a bolus placed on the treatment couch. (i) and (ii) are placed at positions where they do not block the X-rays used by the tumor-monitoring system. Three patients with different tumor sizes (22-682 ml) were examined.

In option (i), the average treatment time, calculated over 8 respiratory patterns, were 54-78% of option (ii) and 52-73% of option (iii). On the other hand, the differences of CTV D5% and D95% between options (i)-(iii) were 1% at maximum. Normal liver V20GyE was smallest in option (iii) and was increased by 1-2% in option (ii) and (iii). No difference (<0.5%) was observed between (ii) and (iii).

In summary, treatment time could be reduced to a great extent by using a mini ridge-filter while only a subtle degradation of DVHs were observed compared to the treatment using a bolus. Considering that the use of a bolus may increase the X-ray exposure dose and the complexity of treatment workflow, we conclude that the mini ridge-filter option is useful for treating the shallow-seated liver tumors with a real-time gating system.

### 15) New prospective and practical 4DCT

Tinsu Pan, PhD

*University of Texas MD Anderson Cancer Center, Department of Imaging Physics*

**Purpose:** It was reported that 90% of the 4DCT patient studies and 30% of the lung or mediastinal tumors were with at least one artifact caused by irregular respiration in a study of 50 patients. A prospective 4DCT based on real-time monitoring of the respiratory signal was proposed on a single-slice Philips PQ-5000 scanner to fix the problem by Keall et al in 2007. However, there has been no progress to make prospective 4DCT available in the modern multi-slice CT scanners (MSCT). To fill this void, we have proposed a new prospective and practical 4DCT without any addition of hardware or software on MSCT.

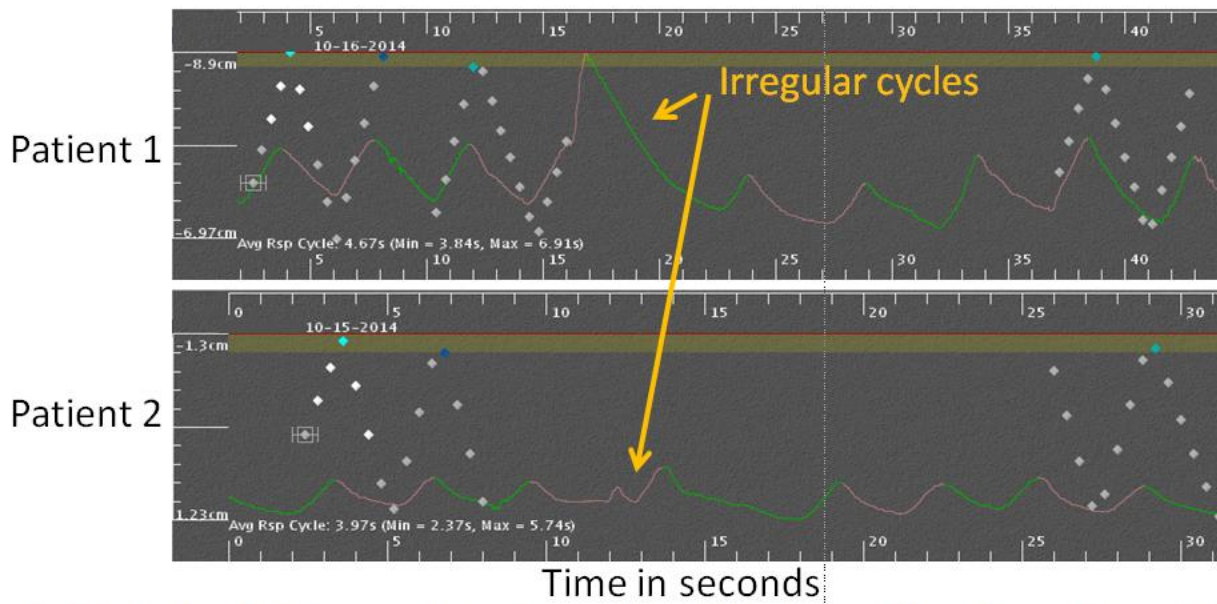
**Methods:** We utilize the independence property of the cine CT scans in the design of the new prospective cine 4DCT. During the cine-CT scan of each position, the scan can be stopped for an irregular respiration and can be resumed when the respiration becomes regular. This process can be repeated as many times as needed. A retrospective cine CT image reconstruction will be initiated after the scan to remove the incomplete cine acquisitions with the irregular respiratory cycles. The end result is a 4DCT free of irregular respiration. We conducted an IRB protocol to recruit 10 patients to prove this concept.

**Results:** Two of the 10 patients exhibited an irregular respiratory cycle during 4DCT, and their 4DCT data acquisitions were stopped due to the irregularities, and resumed when their respiration became normal. The artifacts associated with the irregular respiratory cycles were removed in both patients.

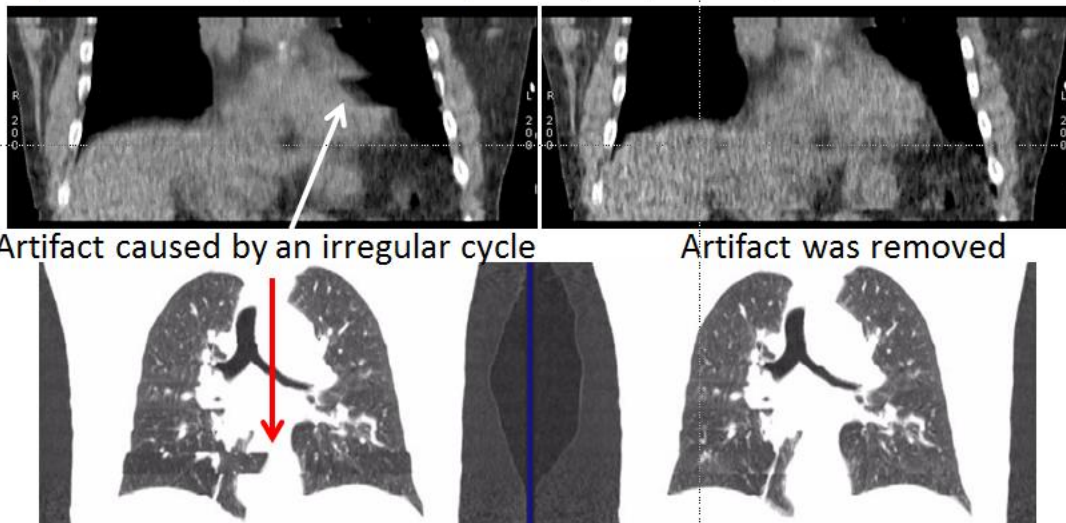
**Conclusion:** We have proposed a new prospective 4DCT scan and processing technique to remove the irregular respiratory cycles and to mitigate their impact to the 4DCT imaging. The technique can be practiced in the 4DCT on the GE MSCT scanners without any addition of hardware or software.

**Innovation/Impact:** We have designed the first prospective 4DCT that can be implemented without any addition of hardware or software in the clinic.

**Key Results:** The irregular respiratory cycles in two of the 10 patients in an IRB study were effectively removed in the following two examples.



Each diamond indicates one CT reconstruction. The diamonds on the positive and negative slopes are in inspiration and expiration, respectively.



## 16) Comparison of 4DCT retrospective reconstruction with two different motion monitoring systems

Riccardo Via<sup>1</sup>, Andrea Pella<sup>2</sup>, Silvia Molinelli<sup>2</sup>, Matteo Seregni<sup>1</sup>, Marco Riboldi<sup>1</sup>, Francesca Valvo<sup>2</sup>, Mario Ciocca<sup>2</sup>, Sandro Rossi<sup>2</sup>, Roberto Orecchia<sup>2,3,4</sup>, Guido Baroni<sup>1,2</sup>

<sup>1</sup>Politecnico di Milano, Department of Electronics Information and Bioengineering, Milano, Italy, <sup>2</sup>CNAO Foundation, Clinical Division, Pavia, Italy, <sup>3</sup>University of Milan, Milano, Italy, <sup>4</sup>European Institute of Oncology, Division of Radiotherapy, Milano, Italy

Radiotherapy treatment planning for tumors affected by respiratory motion is commonly based on time-resolved computerized tomography (4DCT). The ANZAI system (Anzai Medical CO.,Ltd), currently used at CNAO, consists in a load cell transducer (fixed on patient's skin) that generates a mono-dimensional signal used as a breathing motion surrogate for retrospective 4DCT reconstruction. To investigate the capabilities of an alternative approach, a dedicated custom-made optical tracking system (OTSCT) is being developed at CNAO.

This study compares the 4DCT dataset acquired using the ANZAI surrogate with those obtained with the OTSCT signal in simultaneous scan. To simulate motion, we used the ANZAI respiratory phantom, featuring three spheres moving with sinusoidal or quasirespiratory waveforms. OTSCT is based on three triggered CMOS cameras able to detect passive markers placed on the moving cylindrical section of the phantom. Separate sets (CT-A for ANZAI and CT-O for OTSCT) of 4DCT in the end-exhale (EE), mid-exhale (ME) and end-inhale (EI) phases were generated retrospectively. The phase of respiratory signals  $[0-2\pi]$  was calculated a posteriori by linear interpolation between adjacent amplitude minima (phase=0). Slice-by-slice semi-automatic segmentation followed by circular fitting was performed on the spheres volume. Compared to a nominal value of 20 mm, a mean (SD) range of motion of 17.03 mm (1.51 mm) and 18.78 mm (0.48 mm) was found in CT-A and CT-O datasets, respectively. Circular fitting error in the range of -1.66 mm/1.80 mm was found in CT-A scans while CT-O dataset were characterized by residuals range of -1.58 mm /1.89 mm.

These results proved the feasibility of retrospective 4DCT reconstruction using OTSCT. Although similar results in terms of sphere circularity were found, phantom motion in the CT-A dataset was underestimated with respect to CT-O. Future activities will extend this analysis to clinical data while further device development will enable multi-dimensional signals acquisition and surface reconstruction.

## 17) Evaluation of differences in the target displacement between X-ray fluoroscopic and four-dimensional cone-beam computed tomography imaging with amplitude- and phase-based sorting

Hiraku Iramina<sup>1,2</sup>, Mitsuhiro Nakamura<sup>2</sup>, Yusuke Iizuka<sup>2</sup>, Yukinori Matsuo<sup>2</sup>, Takashi Mizowaki<sup>2</sup>, Masahiro Hiraoka<sup>2</sup>, Ikuo Kanno<sup>1</sup>

<sup>1</sup>Department of Nuclear Engineering, Graduate School of Engineering, Kyoto University, <sup>2</sup>Department of Radiation Oncology and Image-Applied Therapy, Graduate School of Medicine, Kyoto University

Four-dimensional cone-beam computed tomography (4D-CBCT) has great capability to provide volumetric and respiratory motion information. It is necessary to quantitatively assess how difference of tumor displacement between actual and 4D-CBCT image exists. In this study, we evaluated the displacement of implanted fiducial markers on fluoroscopic projection images and reconstructed 4D-CBCT images with two different sorting methods.

We have developed 4D-CBCT utilizing dual source kV X-ray imaging subsystems. Five lung cancer patients with two to four implanted fiducial markers were enrolled in the institutional review board-approved trial. 4D-CBCT data were acquired with a voxel size of  $1 \times 1 \times 1 \text{ mm}^3$ . The maximum field of view was 200 mm in diameter and 150 mm in length, and the imaging parameters were 110 kV, 160 mA and 5 ms. The rotational angle, speed, and rotation time of the gantry were  $105^\circ$ ,  $1.5^\circ/\text{s}$ , and 70 s. The marker motion in superior-inferior (SI) direction, which located the most nearest to the lung tumor, was used as surrogate respiratory signal for 4D-CBCT image reconstruction. The signal was converted to eight phase bins with retrospective amplitude- or phase- based sorting. On reconstructed 4D-CBCT images, the marker was contoured on all phases to detect its 3D positions. Meanwhile, the marker positions on two fluoroscopic images obtained at the same time were converted to 3D position. Evaluation was employed among the displacement on fluoroscopic image ( $d_{\text{fluoro}}$ ), that on amplitude- ( $d_{\text{a-4DCBCT}}$ ) and that on phase-based sorting 4D-CBCT ( $d_{\text{p-4DCBCT}}$ ) in left-right (LR), anterior-posterior (AP), and SI direction. Difference between  $d_{\text{a-4DCBCT}}$  and  $d_{\text{fluoro}}$  ( $D_{\text{a-f}}$ ), and that between  $d_{\text{p-4DCBCT}}$  and  $d_{\text{fluoro}}$  ( $D_{\text{p-f}}$ ) were obtained for all patients.

Mean of  $D_{\text{a-f}}$  and  $D_{\text{p-f}}$  for LR, AP, and SI direction were -1.6, -2.4, -5.2 mm and -1.5, -1.9, -4.9 mm, respectively. Note that 4D-CBCT underestimates displacement of markers by 5 mm in SI direction on average since 4D-CBCT requires convolution of marker motion in eight bins.

### 18) Real time tracking by CyberKnife and Vero in liver SBRT: dosimetric comparison by planning structure-based $\gamma$ -evaluation and dose-area-histograms

T. Sothmann<sup>1,5</sup>, O. Blanck<sup>2,3</sup>, K. Poels<sup>4</sup>, R. Werner<sup>5</sup>, T. Gauer<sup>1</sup>

<sup>1</sup>Department of Radiotherapy and Radio-Oncology, University Medical Center Hamburg-Eppendorf, Hamburg, Germany, <sup>2</sup>Department of Radiation Oncology, University Medical Center of Schleswig-Holstein, Kiel, Germany, <sup>3</sup>Saphir Radiosurgery Center Frankfurt and Güstrow, Germany, <sup>4</sup>Radiotherapy Department, Vrije Universiteit Brussel, Belgium, <sup>5</sup>Department of Computational Neuroscience, University Medical Center Hamburg-Eppendorf, Hamburg, Germany

In this study two clinical tracking systems for radiosurgery were evaluated and compared with respect to their dosimetric and geometrical accuracy in liver SBRT: the gimbal-based Vero and the robot-based CyberKnife. The approaches of Vero and CyberKnife perform real-time tumour tracking by correlating internal tumour and external surrogate motion.

CyberKnife treatment plans were delivered to a high resolution 2D detector array mounted on a 4D motion platform to simulate (a) tumour motion trajectories extracted from the corresponding CyberKnife predictor log files and (b) the tumour motion trajectories with superimposed baseline drift. Relevant uncertainties of dosimetric and geometrical parameters were determined by analyzing static reference and tracked dose measurements using a planning structure-based evaluation method.

Inside the CTV  $\gamma$ -passing rates ( $\gamma$ -criteria of 1% / 1 mm) ranged from 95% to 100% (CyberKnife) and 98% to 100% (Vero) for case (a). Dosimetric accuracy decreases in the presence of the baseline drift. Tracked dose measurements resulted in  $\gamma$ -passing rates from 26% to 92% and 94% to 99% for case (b), respectively. The effect was more pronounced for CyberKnife, whereas the Vero system led to maximum dose deviations in the OAR between +1.5 Gy to +6.0Gy (CyberKnife: +0.5 Gy to +3.5 Gy). Dose shifts were interpreted as motion-induced geometrical tracking errors. Maximum observed shift ranges were -1.0 mm to +0.7 mm (lateral) / -0.6 mm to +0.1 mm (superior-inferior) for CyberKnife and -0.8 mm to +0.2 mm / -0.8 mm to +0.4 mm for Vero.

The present work demonstrates that CyberKnife and Vero allow for high precision tracking of regular breathing patterns. The obtained dose distributions appear to be clinical acceptable with regard to literature QA  $\gamma$ -criteria of 3% / 3 mm.

## 19) Monitoring of respiratory motion: comparative analysis of optical and electromagnetic solutions

G. Fattori<sup>1</sup>, S. Safai<sup>1</sup>, P. Fernández Carmona<sup>1</sup>, M. Peroni<sup>1</sup>, R. Perrin<sup>1</sup>, D. C. Weber<sup>1</sup>, A. J. Lomax<sup>1</sup>

<sup>1</sup>Center for Proton Therapy, Paul Scherrer Institut, 5232 Villigen PSI

**Purpose:** to investigate benefits and pitfalls of non-invasive respiratory motion monitoring by means of optical and electromagnetic tracking technologies.

**Methods:** motion data captured with the Polaris SPECTRA optical tracking system (OTS) and Aurora V3 electromagnetic tracking system (EMTS) from Northern Digital Inc. (Waterloo, CA) were studied. Static and dynamic distortions have been quantified under controlled laboratory conditions. In addition, a respiratory phantom (Anzai Medical Co., Ltd, Tokyo, Japan) has been used to assess the systems' latency while tracking a realistic respiratory motion pattern. Finally, the two major causes of tracking failure, respectively marker visibility and magnetic field distortions, have been investigated in a clinical environment for a proton therapy gantry system. Effective motion monitoring has also been verified during CT imaging and treatment conditions, mimicking lung proton therapy by means of an anthropomorphic thorax phantom.

**Results:** the spatial jitter of optical measurements was consistently below 0.06 mm (root-mean-square error, RMSE) in the whole working volume, whereas the precision of EMTS dropped from 0.05 mm to 0.2 mm RMSE with increasing distance from the EM antenna. Similarly, higher dynamic distortions were observed with the EMTS (2.83 mm RMSE) compared to the OTS (0.33 mm RMSE). The average latency for respiratory motion tracking was  $16.6 \pm 0.9$  msec and  $31.6 \pm 1.0$  msec (mean $\pm$ std.dev.) for the Polaris and Aurora systems, respectively.

In worst-case conditions, the nozzle occluded the view of upper chest landmarks. Instead, the application of electromagnetic tracking, albeit overcoming the line-of-sight restriction, is critically limited by nearby diagnostic devices. Specifically, three main sources of distortion contribute to reduction of tracking accuracy during imaging: the distance between the CT gantry and the magnetic field generator (up to 7.3 mm), the rotation of the CT gantry (up to 25 mm) and activation of the X-ray source (up to 3 mm). Similarly, the presence of the treatment nozzle within the measurement workspace affects sensor localization.

**Conclusion:** optical and electromagnetic tracking systems were compared for respiratory motion monitoring in radiotherapy. At the current stage of technology, the optical solution offers the greatest potential, being robust against environmental factors and providing high spatial accuracy.

The research leading to these results has received funding from the European Community's Seventh Framework Programme (FP7/2007-2013) under grant agreement n.°290605 (PSI-FELLOW/COFUND).

## 20) Geometric and dosimetric validation of motion monitoring techniques in respiratory-gated radiotherapy using a dynamic lung phantom in combination with dosimetry gels

P. Mann<sup>1</sup>, M. Witte<sup>1</sup>, T. Moser<sup>1</sup>, C. Lang<sup>1</sup>, A. Runz<sup>1</sup>, M. Berger<sup>2</sup>, J. Biederer<sup>3</sup>, C.P. Karger<sup>1</sup>

<sup>1</sup>Department of Medical Physics in Radiation Oncology, German Cancer Research Center, INF 280, 69120 Heidelberg, Germany, <sup>2</sup>Department of Medical Physics in Radiology, German Cancer Research Center, INF 280, 69120 Heidelberg, Germany, <sup>3</sup>Department of Diagnostic and Interventional Radiology, Section of Pulmonary Imaging, University of Heidelberg, INF 110, 69120 Heidelberg, Germany

A dynamic ex-vivo porcine lung phantom combined with in-house produced and evaluated polymer dosimetry gel (PAGAT) was tested as a new tool for geometric and dosimetric verification of modern adaptive photon radiotherapy techniques (e.g. gating) in presence of organ motion. The phantom consists of a PMMA container simulating the thorax, which contains a post mortem explanted porcine lung, which can move in arbitrary breathing patterns. The dosimetry gel consists of monomers, embedded within a gelatin matrix, which polymerize after irradiation. The resulting polymers exhibit a dose-dependent transversal relaxation rate ( $R_2=1/T_2$ ), which can be evaluated in magnetic resonance imaging by using a multi-spin echo sequence. Due to the high reactivity with oxygen and other materials, the gel was stored inside a BAREX© container protecting the gel from chemical reactions. To test the feasibility of 3D-dose measurements inside the phantom, a small spherical dose distribution (3 coplanar and equally-spaced  $1 \times 1 \text{ cm}^2$ -fields), located completely within the gel container was planned and delivered with and without lung phantom motion for a gated and non-gated case. Gel calibration was realized by irradiating a batch of 8 samples with doses of 0 to 7 Gy. To verify clinical treatment concepts, the entire gel volume was considered a tumor and was homogeneously irradiated (9 coplanar fields) using adequate setup margins (ICRU 50) in the static case and by considering an additional 4D CT-based ITV (ICRU 62) in case of the lung phantom motion with and without gating. For quantitative dose evaluation, a denoising filter was applied to the MR data and the mono exponential calibration curve was renormalized. The feasibility test clearly demonstrated the impact of target motion and its compensation by gating. Simulated treatments revealed complete target coverage in all cases. A good agreement between measured and calculated dose was found (83–92% acceptance rate for the gamma-criteria 3 mm/3%). In combination with 3D gel dosimetry, the dynamic lung phantom provides a new and promising tool to validate complex treatment techniques such as gating geometrically as well as dosimetrically.

## 21) A comparison of proton PBS and photon VMAT treatments with film dosimetry in the anthropomorphic lung phantom (LuCa)

Rosalind Perrin<sup>1</sup>, Stefanie Ehrbar<sup>2,3</sup>, Marta Peroni<sup>1</sup>, Kinga Bernatowicz<sup>1</sup>, Thomas Parkel<sup>4</sup>, Izabela Pytko<sup>2,3</sup>, Stephan Klöck<sup>2,3</sup>, Damien Charles Weber<sup>1</sup>, Tony Lomax<sup>1</sup>, Matthias Guckenberger<sup>2,3</sup>, Stephanie Lang<sup>2,3</sup>

<sup>1</sup>Paul Scherrer Institute, 5232 Villigen PSI, Switzerland, <sup>2</sup>Department of Radiation Oncology, University Hospital Zurich, 8091 Zürich, Switzerland, <sup>3</sup>University of Zurich, Zürich, Switzerland, <sup>4</sup>CSEM Centre Suisse d'Electronique et de Microtechnique SA, Innovative Design, Landquart, Switzerland

**Purpose:** To verify dose distributions resulting from lung cancer irradiation strategies between pencil beam scanned (PBS) proton therapy and photon treatments with volumetric modulated arc therapy (VMAT).

**Methods:** Two institutions participated in this dose verification study for motion-mitigated lung treatments: the Center for Proton Therapy at the Paul Scherrer Institute (PSI) and the Department of Radiation Oncology, University Hospital Zurich. The dynamic, anthropomorphic, breathing phantom, LuCa, was operated with 5 different respiration patterns, including sin and sin<sup>4</sup> patterns at 10 mm and 20 mm total excursion (peak-to-peak amplitude), and a patient specific breathing curve with 15 mm maximum excursion (range 10-15 mm). A wooden sphere was used to emulate a tumour in the right-side of the lung. 4DCT scans were taken and VMAT and proton PBS treatment plans were prepared. The PTV was generated from the averaged CT calculated from a 4DCT scan, and was the total motion envelope of the target (geometric ITV). The CTV was the PTV with a negative margin of 0.5 cm. This was done so that the all proton beam spots were placed within the wooden sphere. A dose of 2 Gy was prescribed to the mean dose in the PTV.

For the proton plan, 3 fields were generated at gantry angles -27°, 16° and 63° (see Fig. 1a). So that pencil beams of range matching the distal edge of the target at all positions in its motion path, the PTV was overridden with the Hounsfield unit (HU) measured for the wooden target. 10 rescans were applied for the patient and 1 cm motion patterns and 15 rescans for the 2 cm motion patterns in the PBS deliveries. For the photon irradiations, VMAT plans were optimized with 2 full arcs and with dose constraints to the lung, heart and spinal cord.

Gafchromic film was inserted into 2 planes of the spherical wooden target prior to each delivery for a given motion pattern. Measurements of dose to normal tissues were also performed (see Fig 1), i) to the heart (model heart containing a single film plane) and ii) to a point (ionisation chamber) adjacent to the spine, measuring dose to tissue distal to the target.

**Results:** Table 1 shows the dose statistics for the films in the CTV, and Table 2 the measurements for the heart film and ionisation chamber. For the 1 cm total excursion sine pattern and static cases both treatment modalities gave a clinically acceptable dose distribution to the CTV ( $V_{95} > 99\%$ ,  $D_{95} > 95\%$  and  $D_5-D_{95} < 10\%$ ). VMAT treatment produced better coverage of the moving target for the remaining cases. However, some interplay was observed with VMAT for the patient-specific- ( $V_{107} = 11.3\%$ ) and 2 cm-sin-pattern cases ( $V_{95} = 91.1\%$ ). For PBS, the 2 cm motion pattern cases were lower in mean dose ( $< 98\%$ ),  $D_{95}$  ( $< 95\%$ ) and  $V_{95}$  ( $< 92\%$ ), while maintaining an acceptable homogeneity ( $D_5-D_{95} < 7\%$ ). This indicates a dose smearing effect over the rescans, and could be potentially compensated by a boosting of the treatment plan.

Organ at risk doses were similar in both treatment modalities for the heart, but 1.5 – 3 times higher in PBS at the chamber adjacent to the spine. This was due to the planning technique, whereby the pencil-beam range was matched to the distal edge of the PTV by overriding the HU to the full motion excursion of the target. Thus some Bragg peaks of the pencil beams reached the chamber at time points when the target was not in line with the pencil beam.

**Conclusion:** While a small amount of interplay was measured at 2 cm motion, VMAT performed well under the test conditions. PBS dose distribution proved to be more sensitive to motion, but motion mitigation was adequate for 1 cm total motion with 10 times rescanned PBS. Ongoing work on proton PBS treatments in lung is being focussed towards i) beam gating and ii) improving the planning technique for rescanned PBS, using range-adaptive ITV and 4D optimisation, so that beam overshoot into normal tissues is minimised.

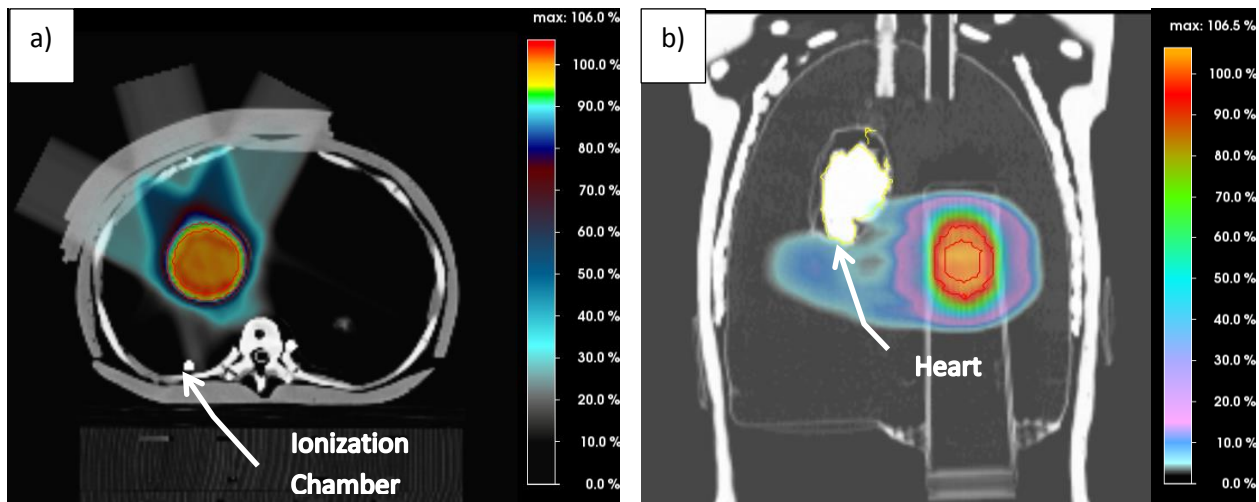


**Figure 1:** Proton PBS treatment plan showing measurement positions of the a) chamber and b) the heart with respect to the applied fields.

**Table 1:** Dose measurements to the CTV for planned dose distribution (in bold), and measured static control and motion cases (n.d. = no data). Dose is normalised to the mean dose measured in the “1cm ITV” or “2cm ITV” static control case as appropriate in PBS, and the static control for the “1cm ITV” plan in photons.

Total motion (cm) and case	Dmean (%)		D95 (%)		D5 (%)		Hom5-95 (%)		V95 (>1.9Gy) (%)		V107 (>2.14Gy) (%)	
	VMAT	PBS	VMAT	PBS	VMAT	PBS	VMAT	PBS	VMAT	PBS	VMAT	PBS
<b>Planned 1cm ITV</b>	<b>100.1</b>	<b>100.9</b>	<b>99.0</b>	<b>99.8</b>	<b>101.1</b>	<b>104.4</b>	<b>2.0</b>	<b>4.6</b>	<b>100.0</b>	<b>100.0</b>	<b>0.0</b>	<b>0.0</b>
0.0 Static 1cm ITV	100.0	100.0	97.3	96.9	103.0	103.1	5.7	6.2	99.8	99.9	0.0	0.1
1.0 sin	102.7	100.9	99.1	96.0	106.7	103.8	7.4	7.8	100.0	98.1	3.9	0.2
1.0 sin4	100.9	100.9	97.5	96.3	104.4	103.0	6.8	6.7	100.0	99.4	0.0	0.1
<b>Planned 2cm ITV</b>	<b>100.1</b>	<b>101.6</b>	<b>99.1</b>	<b>99.6</b>	<b>100.9</b>	<b>103.7</b>	<b>1.8</b>	<b>4.1</b>	<b>100.0</b>	<b>100.0</b>	<b>0.0</b>	<b>0.4</b>
0.0 Static 2cm ITV	n.d.	100.0	n.d.	96.3	n.d.	103.1	n.d.	6.8	n.d.	98.3	n.d.	0.0
2.0 sin	99.7	98.1	94.0	94.3	105.5	101.2	11.5	6.9	91.2	92.3	1.5	0.0
2.0 sin4	104.0	97.6	100.4	93.9	107.7	101.1	7.1	7.2	100.0	89.2	9.7	0.0
1.4 Patient	102.1	100.9	96.1	91.8	109.0	102.1	12.6	10.3	99.1	84.5	11.3	0.1

**Table 2:** Dose measurements to 2 measurement points in normal tissues (n.d. = no data)

Total motion (cm) and case	Heart (Film)		Spinal Cord (Chamber)	
	Dmean (Gy)		Dmean (Gy)	
	VMAT	PBS	VMAT	PBS
<b>Planned 1cm ITV</b>	<b>0.06</b>	<b>0.00</b>	<b>0.66</b>	<b>0.17</b>
1.0 sin	0.04	0.04	0.69	1.08
1.0 sin4	0.02	0.09	0.65	0.99
<b>Planned 2cm ITV</b>	<b>0.09</b>	<b>0.00</b>	<b>0.61</b>	<b>0.18</b>
2.0 sin	0.09	0.09	0.54	1.68
2.0 sin4	0.09	0.09	0.70	1.61
1.4 Patient	0.09	n.d.	0.70	1.01

## 22) Measurements and simulations of charged secondary production in view of pre-clinical tests of in-vivo monitoring system for ion beam therapy

A. Rucinski<sup>1,2</sup>, G. Battistoni<sup>3</sup>, F. Collamati<sup>1,4</sup>, E. De Lucia<sup>5</sup>, R. Faccini<sup>1,4</sup>, M. Marafini<sup>1,4</sup>, I. Mattei<sup>3</sup>, S. Muraro<sup>3</sup>, R. Paramatti<sup>1</sup>, V. Patera<sup>1,2,6</sup>, D. Pinci<sup>1</sup>, A. Russomando<sup>1,4,7</sup>, A. Sarti<sup>2,5,6</sup>, A. Sciubba<sup>1,2,6</sup>, E. Solfaroli Camillocci<sup>4</sup>, M. Toppi<sup>5</sup>, G. Traini<sup>1,4</sup>, C. Voena<sup>1,4</sup>

<sup>1</sup>INFN Sezione di Roma, Roma, Italy, <sup>2</sup>Dipartimento di Scienze di Base e Applicate per Ingegneria, Sapienza Universit`a di Roma, Roma, Italy, <sup>3</sup>INFN Sezione di Milano, Milano, Italy, <sup>4</sup>Dipartimento di Fisica, Sapienza Universit`a di Roma, Roma, Italy, <sup>5</sup>Laboratori Nazionali di Frascati dell'INFN, Frascati, Italy, <sup>6</sup>Museo Storico della Fisica e Centro Studi e Ricerche "E. Fermi", Roma, Italy, <sup>7</sup>Center for Life Nano Science@Sapienza, Istituto Italiano di Tecnologia, Roma, Italy

In scanned ion beam therapy one of the main effort is made in the development of on-line assessment of the beam delivery accuracy. In particular, for application of unconventional treatment protocols like unusual irradiation fields, hypo-fractionation, etc, the online monitoring of the dose delivery is crucial. Monitoring techniques that exploit the secondary particles produced by the interaction of the beam with the patient must provide the accurate information on the position of the beam entrance into the patient. Furthermore the correlation of the emission profile of secondary particles with the position of the Bragg-peak could be an online indication on anatomy variations, TPS re-planning or adaptive treatment procedures.

This contribution reports on measurements performed at HIT (Heidelberg, Germany) facility and their implications for the development of the on-line monitoring system for ion beam therapy. At HIT the secondary particles produced by 12C, 4He and 16O ion beams of therapeutic energies impinging on PMMA phantoms have been studied at different angular configurations with respect to the primary beam. The emission energy spectra, yields of secondary fragments as well as the spatial distribution at production (emission profiles) were obtained, as they are not accurately predicted by the available MC codes. The correlation between the secondary emission region and Bragg Peak position will be shown demonstrating the feasibility of range monitoring using charged secondary particles. As the number of secondary particles reaching the detector depends on primary beam energy, number of particles delivered to the raster point and the distance that the particle has to travel before exiting patient tissue and reaching the detector, the prediction of the performance of the on-line monitoring system in the clinical conditions is a complex problem. This contribution presents the design and reports on the status of development of a real time dose monitoring system prototype Dose Profiler, which is planned to be tested in spring 2016. The detector consists of charged secondaries tracker composed of scintillating fiber layers and LYSO calorimeter for measurement of particles energy read-out by front end electronics and FPGA boards. The DAQ design allows data taking with the acquisition rate greater than the expected secondary particles rate, which should allow to compare expected and actual emission profile raster point by raster point. Using as input the data obtained at HIT, the simulation of the charged secondary protons emitted from a spherical phantom is currently studied and a preliminary example of the on-line detector response in such a scenario will be shown.

### 23) Real-time Tracking of Liver Landmarks in 2D Ultrasound Sequences

Maxim Makhinya and [Orçun Gökse](#)

*Computer-assisted Applications in Medicine, ETH Zürich, Switzerland*

Planned delivery of focused therapy is adversely affected by internal body motion, such as from breathing, which could be mitigated, if tracked accurately in real-time. By extending an algorithm for superficial vein tracking [1], we have recently presented a robust real-time motion tracking method for 2D ultrasound image sequences of the liver [2]. The method leverages elliptic and template-based models of vessels in the liver, coupled with a robust optic-flow framework resulting in iterative tracking. Potential drifts are corrected when the breathing phase is close to that of the initial reference frame, detected by comparing the appearance of tracked feature regions.

Our method runs on a standard computer in real-time with latencies of 20-70 ms. It is implemented as a mobile platform to be connected from the display output of any ultrasound machine in clinics [1]. Performance of our technique has been evaluated through the MICCAI Challenge on Liver Ultrasound Tracking (CLUST) 2015 [2]. This benchmark consisted of 64 2D ultrasound sequences (test-set with an average resolution of 447x552 px and an average length of 3761 frames at ~15 fps) collected from four institutes. For evaluation, up to 4 landmarks were selected in several frames by 3 different observers. Our method resulted in 1.09 (1.75) mm mean(std) error with 95th percentile at 2.42 mm, while the three annotators' mean difference from their averaged consensus location was 0.5 mm with 95<sup>th</sup> percentile at 1 mm.

Our system can be easily incorporated into the treatment room for real-time tracking of liver motion in 2D. Extension to 3D will be investigated next.

[1] A.Crimi, M.Makhinya, U.Baumann, C.Thalhammer, G.Szekely, O.Goksel: "Automatic Measurement of Venous Pressure Using B-Mode Ultrasound", IEEE Trans Biomed Eng, 2015.

[2] M.Makhinya, O.Goksel: "Motion Tracking in 2D Ultrasound Using Vessel Models and Robust Optic-Flow", In MICCAI Challenge on Liver Motion Tracking (CLUST), 2015.

## 24) Ultrasound and MR-Tracking for Intra-Fractional Motion Compensation in Radiation Therapy

Jürgen Jenne<sup>1,2</sup>, Sven Rothlübbers<sup>1,2</sup>, Julia Schwaab<sup>2</sup>, Steffen Tretbar<sup>3</sup>, Matthias Günther<sup>1,2</sup>

<sup>1</sup>Fraunhofer-Institut für Bildgestützte Medizin (MEVIS), Bremen, <sup>2</sup>mediri GmbH, Heidelberg, <sup>3</sup>Fraunhofer-Institut für Biomedizinische Technik (IBMT), St. Ingbert

There is an undiminished necessity for precision in radiation therapy. Particle and intensity modulated photon radiation therapy enable treatment accuracies within millimeter scale under static conditions. Target motion however - particularly in the abdomen, due to respiration or patient movement - is still a challenge and demands methods that detect and compensate it. Diagnostic ultrasound (US) and magnetic resonance (MR) imaging represent non-invasive, dose-free and model-independent alternatives to implants, fluoroscopy, respiration belt or optical tracking.

For several years mediri, MEVIS and IBMT are working on ultrasound based motion tracking for radiation therapy. In this context, e.g. a dedicated US-tracking system was designed and build. It was equipped with a customized probe which allows interleaved imaging of two perpendicular planes to enable quasi 3D tracking in real-time with high position update rates. In addition, a reliable tracking algorithm based on conditional density propagation was developed, which is able to follow manually segmented structures on both image planes independently. In cooperation with GSI, Darmstadt and HIT, Heidelberg, motion compensation with actively scanned heavy ions based on our real-time US motion detection was demonstrated [1, 2].

Both US tracking hardware and software are continuously being improved. The image based tracking software was adapted and modified for MR based motion tracking. To improve the tracking software for both MR and US, landmark based tracking method was developed in addition to the existing contour tracking [3]. Automated landmark detection and a method to identify the quality of the tracking result complement the software. Accuracy of the ongoing developments was measured on US image streams and on fast MR-EPI images from GE scanners. Evaluation showed an average error of 1.52 mm for US and 2.2 mm/1.7 mm for MR tracking in liver images [4, 5]. Future US-hardware, developed by our partner IBMT, will be MR compatible and include fast plane wave imaging allowing frame rates over 100 Hz.

### Literature

- [1] M. Prall, R. Kaderka, N. Saito, C. Graeff, C. Bert, M. Durante, K. Parodi, J. Schwaab, C. Sarti, J. Jenne, Ion beam tracking using ultrasound motion detection, *Medical Physics*, 41 (2014) 041708.
- [2] J. Schwaab, M. Prall, C. Sarti, R. Kaderka, C. Bert, C. Kurz, K. Parodi, M. Gunther, J. Jenne, Ultrasound tracking for intra-fractional motion compensation in radiation therapy, *Physica medica : PM : an international journal devoted to the applications of physics to medicine and biology : official journal of the Italian Association of Biomedical Physics*, 30 (2014) 578-582.
- [3] S. Rothluebbers, J. Schwaab, J. Jenne, M. Günther, Bayesian Real-Time Liver Feature Ultrasound Tracking, MICCAI workshop: Challenge on Liver Ultrasound Tracking, 2014, pp. 45-52.
- [4] V. De Luca, T. Benz, S. Kondo, L. Konig, D. Lubke, S. Rothluebbers, O. Somphone, S. Allaire, M.A. Lediju Bell, D.Y. Chung, A. Cifor, C. Grozea, M. Gunther, J. Jenne, T. Kipshagen, M. Kowarschik, N. Navab, J. Ruhaak, J. Schwaab, C. Tanner, The 2014 liver ultrasound tracking benchmark, *Physics in medicine and biology*, 60 (2015) 5571-5599.
- [5] S. Rothluebbers, C. Tanner, Y. Zur, K. French, M. Schwenke, J. Strehlow, G. Sat, J. Jenne, M. Günther, Particle filter based liver motion tracking for MRgFUS, *EUFUS Symposium*, 2015.

Parts of the research leading to these results have received funding from the European Community's Seventh Framework Programme FP7/2007-2013 under grant agreement n° 611889.

## 25) The 2015 Challenge on Liver Ultrasound Tracking

Valeria De Luca<sup>1</sup>, Jyotirmoy Banerjee<sup>2,3</sup>, Muyinatu A. Lediju Bell<sup>4</sup>, Andre Hallack<sup>5</sup>, Satoshi Kondo<sup>6</sup>, Maxim Makhinya<sup>1</sup>, Daniel Nouri<sup>7</sup>, Lucas Royer<sup>8,9,10</sup>, Anthony Le Bras<sup>8,11</sup>, Amalia Cifor<sup>12</sup>, Guillaume Dardenne<sup>8</sup>, Emma Harris<sup>13</sup>, Orcun Goksel<sup>1</sup>, Mark J. Gooding<sup>12</sup>, Camiel Klink<sup>2</sup>, Alexandre Krupa<sup>8,9</sup>, Maud Marchal<sup>8,10</sup>, Adriaan Moelker<sup>2</sup>, Wiro J. Niessen<sup>2,3</sup>, Bartlomiej W. Papiez<sup>3</sup>, Alex Rothberg<sup>7</sup>, Julia A. Schnabel<sup>14</sup>, Erwin Vast<sup>2,3</sup>, Theo van Walsum<sup>2,3</sup>, Christine Tanner<sup>1</sup>

<sup>1</sup>Computer Vision Laboratory, ETH Zurich, Switzerland, <sup>2</sup>Department of Radiology, Erasmus MC, Rotterdam, The Netherlands, <sup>3</sup>Department of Medical Informatics, Erasmus MC, Rotterdam, The Netherlands, <sup>4</sup>Engineering Research Center for Computer-Integrated Surgical Systems and Technology, Johns Hopkins University, Baltimore, USA, <sup>5</sup>Institute of Biomedical Engineering, University of Oxford, UK, <sup>6</sup>Konica Minolta Inc., Osaka, Japan, <sup>7</sup>Catalyzer Inc., Guilford CT, USA, <sup>8</sup>Institut de Recherche Technologique b-com, Rennes, France, <sup>9</sup>Inria Rennes - Bretagne Atlantique, France, <sup>10</sup>INSA de Rennes, France, <sup>11</sup>CHU de Rennes, France, <sup>12</sup>Mirada Medical, Oxford, UK, <sup>13</sup>Institute of Cancer Research, London, UK, <sup>14</sup>Division of Imaging Sciences & Biomedical Engineering, King's College London, UK

Ultrasound imaging is the modality of choice for tracking motion during therapy due to its high temporal resolution, non-invasiveness, soft tissue contrast and cost-efficiency. Accurate tracking of the target motion during free-breathing is vital in therapy guidance. The MICCAI 2014 Challenge on Liver Ultrasound Tracking (CLUST 2014) enabled the first direct comparison of the performance of several automated methods for tracking in therapy guidance. In this abstract, we report the results on a subsequent benchmark, CLUST 2015 (<http://clust.ethz.ch/>), which provided a larger dataset (+60%), more manual annotations (three observers, 10% images, quality check), and an on-site challenge.

The database included a total of 86 ultrasound sequences (64 2D and 22 3D) of the liver of healthy volunteers under free-breathing, acquired in six institutes and using seven scanners. The data were divided into a training set (40%, all annotations given), an off-site test set (40%, annotations for first frame given), and an on-site test set (20%, provided during MICCAI event). The data were downloaded ~50 times and tracking results for the off-site test set were submitted by eight groups for evaluation by the organizers. We compared the six methods which finally participated in the challenge. As an additional method, a fusion (median) of the results of each of the tracking methods was also evaluated.

Quantitative evaluation was performed with respect to the mean annotations of the observers. Results of all methods for the off-site test data showed a mean (95%) tracking error in the range of [0.9,2.8] mm ([2.2,13.1] mm) for 2D landmarks, and [1.5,1.6] mm ([2.4,2.9] mm) for 3D. The 3D 95% errors were lower than the inter-observer errors ([3.0, 3.5] mm). Fusing all 2D automatic results improved the mean (95%) error to 0.7 mm (<2.0 mm).

The most accurate approaches outperformed the ones from CLUST 2014. The small 95% tracking errors demonstrate that these methods can be used to robustly estimate the landmark motion, and therefore have great potential to reduce treatment margins in radiotherapy.

**Acknowledgements:** We thank Anastasia K. Ostrowski and Alicia B. Dagle<sup>4</sup>, Tuathan O'Shea and Srikanta Sharma<sup>13</sup>, Julia Schwaab (mediri GmbH, Germany), and Hervé Liebgott and Adeline Bernard (CREATIS, Lyon, France) for annotating part of the data, and all funding agencies as listed in the MICCAI proceedings

## 26) Estimation of tracking confidence and its use for gated-tracking

Valeria De Luca, Gábor Székely, [Christine Tanner](#)

*Computer Vision Laboratory, ETH Zürich, Switzerland*

Image-guided radiation therapy during free-breathing requires estimation of the target position and compensation for its motion. Quantification of the observed motion during therapy via tracking needs to be reliable and accurate. We devised a novel, image sequence-specific confidence measure to predict the reliability of the tracking results. This method is based on learning the sequence-specific statistical relationship between the image similarities and the displacements of anatomical landmarks from the first breathing cycles. During the real-time treatment phase, the confidence for the tracking results is derived from the relative closeness to the expected values.

The proposed method was first applied to the results of a learning-based tracking algorithm. Assessment consisted of nine 2D B-mode ultrasound sequences of healthy volunteers under free-breathing (3-10 min, 14-25 Hz). For the 15 annotated vessel centres, tracking reduced the mean motion from 5.2 mm to 0.9 mm. Considering only results with sufficiently high confidence (as determined on an independent dataset), the mean (95%) tracking error on the test data was further reduced by 12% (16%), while duty cycle remained sufficiently high (60%).

A similar performance was obtained on ten 2D liver MR sequences (7 min, 3 Hz) for a deformable registration method (20 annotated vessel centres, 12% reduction of the 95% tracking error, duty cycle 74%). This shows the applicability of the method to a different image modality. The confidence estimation method was fast (mean runtime of 0.2 ms on a single CPU) and achieved on average clinically acceptable 95% errors of 1.7 mm and 2.3 mm for US and MR, respectively.

## **27) Liver-Rib Motion Model for Predicting Rib Motion during Free-Breathing**

Golnoosh Samei, Gábor Székely, Christine Tanner

*Computer Vision Laboratory, ETH Zurich, 8092 Zurich, Switzerland*

Magnetic resonance guided high intensity focused ultrasound (MRgHIFU) is a new therapy for treating malignant liver tissues. However, ribs in the beam path may compromise an effective and safe treatment. To switch-off HIFU transducer elements to avoid ribs, their positions during free-breathing need to be known. Yet poor visibility of bones in MR and US liver images does currently not allow tracking them in real time. Hence we investigated predicting the motion of ribs from partial liver observations.

First we devised a method for registering ribs in 4D MRIs, which realistically constraints the rib's motion to a centered 3D rotation around its head while also optimizing the head's position to account for patient motion. Optimization was performed over tubular masks around the ribs. Tested on 8 volunteers over 100 breathing cycles during free-breathing, our registration reduced the mean motion from 2.71 mm to 1.06 mm for deep inhalations. Analyzing the extracted ribs' motion, we showed that the main ribs' motion is a single rotation around an axis defined by the ribs head and the articular part of the tubercle. This is the first time the ribs' motion due to respiration has been directly studied during free-breathing over a relatively long time.

Secondly, having extracted the ribs' and the liver motion from the 4D MRIs, we developed subject-specific and population-based statistical motion models, to predict the ribs' motion from the motion of the liver. We showed that only a single rotation correlated well with the liver motion magnitude, whose axis was then employed for inter-subject correspondence. Finally the ribs' motion could be reduced by 60% and 40% by the subject-specific and population model, respectively.

## **28) Prediction of respiratory liver motion via robust exemplar model and individualization from an additional breath-hold image**

Christine Tanner, Golnoosh Samei, Gábor Székely

*Computer Vision Laboratory, ETH Zürich, Switzerland*

Motion models have been developed to predict from partial motion observation the position of the whole organ. These are based on learning the statistical relationship of the motion in different parts of the organ from 4D MR images either subject-specific or for a population. Subject-specific models are more accurate, but the acquisition of 4D MRIs is expensive and time consuming. Instead we propose in this study to employ a population exemplar model and individualize it by the motion pattern extracted from an additional breath-hold image. We also investigated the influence of tracking errors on the model prediction and proposed a robust formulation of the exemplar model.

The methods were tested using 4D MRI data from 16 volunteers, simulated noisy 2D tracking results, simulated breath-holds from the 4D MRIs and leave-one-subject-out tests. For 3 volunteers breath-holds at end-exhalation and end-inhalation were acquired.

The robust formulation of the exemplar model led to mean (95%) prediction improvements of 6% (6%) for tracking errors with 1 mm standard deviation. Individualization by an example 3D motion field from the 4D MRI provided additional improvements (mean: 7%, 95%: 13%).

Similar benefits could be achieved from breath-hold images, after automatically detecting and excluding unsuitable motion examples.

## **29) Respiratory Motion Compensation with Topology Independent Surrogates**

Christoph Jud, Frank Preiswerk, Philippe C. Cattin

*Medical Image Analysis Center (MIAC), Department of Biomedical Engineering, Universität Basel*

We present a novel method for respiratory organ motion compensation based on a statistical motion model, in which the surrogate signals can be independent of the model's topology. Provided that they are correlated to the organ motion these might be a spirometer, a breathing belt or a 1D ultrasound where the sensor is placed on the abdominal skin. The key idea is to predict the parameters of our statistical motion model given the surrogate data using non-linear regression. Thus, the surrogates are decoupled from the topological representation of the model. Besides motion estimation, our method enables the synthesis of a respiratory cycle with a high temporal resolution. This can be used to investigate the patient specific motion pattern for planning.

Our model is an additive superposition of a statistical shape model and a statistical motion model. The shape model is built upon a population of exhalation masters which have been registered. The motion is modeled as a mixture of Gaussian distributions where each component distribution describes the motion pattern of a subject. In this way, all motion samples of each subject are considered. It is parametrized over an orthogonal basis using the first two moments of the mixture. Having given a surrogate signal to each motion measurement we perform Gaussian process regression to establish the relation between the surrogates and the motion model parameters.

In our study with the right liver lobe, on 9 subjects, we simulated a 1D surrogate which indicates the depth of the diaphragm measured from the abdominal skin. With leave-one-out motion models the prediction error is robustly kept below 5 mm, whereas the median stays around 2-3 mm. With patient specific motion models, the average error has been considerably improved to less than 1 mm.

### 30) A Tool for an Interactive Summary of a Radiotherapy Treatment

Christoph Brachmann<sup>1</sup>, Ashley Waring<sup>1</sup>, Grzegorz Chlebus<sup>1</sup>, Florian Weiler<sup>1</sup>, Nadine Traulsen<sup>2</sup>, Stefan Krass<sup>1</sup>

<sup>1</sup>Fraunhofer Institute for Medical Image Computing (MEVIS), Bremen, Germany, <sup>2</sup>Fraunhofer Institute for Medical Image Computing (MEVIS), Lübeck, Germany

**Purpose:** Advanced planning methods in radiotherapy facilitate a more precise radiation delivery, which at the same time demands precise observation and control of the therapy progress. Here, we introduce our current work on a monitoring tool that addresses the main purpose of treatment summary with an interactive and user-friendly interface.

**Methods:** Requirement analysis was performed by means of user-centered design methods. Within the currently running research project SPARTA (funded by BMBF) we have organized regular workshops with radiotherapists and medical physicists from three clinical sites. We identified the most relevant user needs and tested initial paper prototypes or mockups. From that we developed a user interface that allows fast assessment of the progress or the outcome of a radiotherapy course. All required facilities, such as fraction navigation, dose statistics, control imaging, or propagation of contours are arranged according to the main purpose of therapy progress observation. In order to evaluate the capabilities of our concept we are currently implementing a prototype which is being tested with therapy cases provided by our clinical project partners. Due to a highly rated requirement for mobile and quick access we decided to implement the prototype based on a client-server architecture.

**Conclusion:** First evaluations with initial prototypes obtained a positive feedback and clinicians acknowledged our software prototype as highly promising. In particular, a quick visual navigation to every treatment day along with a synchronized view of imaging and propagated structures is much appreciated. Furthermore, portable access to a therapy summary is deemed important for patient care. On the other hand, clinicians wished for a bigger visual focus on therapy progress indicated by anatomical volume changes or dose charts. After further refinements of our prototype we are planning to run quantitative evaluations during the next workshops.

### 31) Compilation of a repeat 4D image database – concept and call for data

R. Werner<sup>1,2</sup>, T. Sothmann<sup>1,2</sup>, T. Gauer<sup>2</sup>

<sup>1</sup>Image Processing/Medical Informatics Group, Department of Computational Neuroscience, <sup>2</sup>Department of Radiotherapy and Radio-Oncology University Medical Center Hamburg-Eppendorf (UKE), Hamburg, Germany

Motion variability is a major source of uncertainty in 4D radiotherapy. Motion-induced target position and shape variability is usually accounted for by an ITV-based treatment planning approach – with the ITV being defined using a single 4D CT of the patient. Reliability of the ITV approach is under debate, but the discussion suffers from a lack of data and detailed knowledge about motion variability on both intra- and inter-fraction levels. As a consequence of a related discussion at the 4D Treatment Planning Workshop 2014 in London, a publicly accessible *repeat 4D image database* is currently being conceptualized. The format is inspired by 4D CT databases ([www.dir-lab.com](http://www.dir-lab.com), [www.creatis.insa-lyon.fr/rio/pop-model](http://www.creatis.insa-lyon.fr/rio/pop-model)) and thought to complement them. Following data categories are intended to be provided:

- 4D MRI data plus (semi-)manually defined landmark correspondence;
- repeat 4D CT data sets plus landmark correspondences and surrogate data associated to the CT data acquisition; and
- pairs of treatment planning 4D CT and 4D CBCT data plus landmark correspondences and surrogate data.

Landmarks provide a commonly accepted basis for evaluation of motion modeling accuracy; surrogate records are considered as being useful in the context of motion modeling, cf. [1,2].

The following parties already agreed on participation in compilation of the database, but further collaboration partners would be highly appreciated: ETH Zürich, University of California Davis, UCLA, and the UKE. It is intended to launch the database as a part of a related MICCAI or ISBI challenge in 2016.

[1] McClelland JR et al: "Respiratory motion models: a review." *Medical Image Analysis* 17:19-42, 2013.

[2] Wilms M et al: "Population-based correspondence models for respiratory motion estimation in the presence of inter-fraction motion variations." In: *Imaging and Computer Assistance in Radiation Therapy – a MICCAI 2015 workshop*, pp. 81-88, 2015.

## LIST OF PARTICIPANTS ...

### ... FROM RESEARCH DEPARTMENTS

Markus Alber	<i>Aarhus University, Denmark</i>
Francesca Albertini	<i>Paul Scherrer Institute, Villigen, Switzerland</i>
Guido Baroni	<i>Politecnico di Milano, Italy</i>
Vania Batista	<i>University Clinic of Heidelberg, HIT, Germany</i>
Michael Baumann	<i>OncoRay, Dresden, Germany</i>
Louise Bendall	<i>CRUK/MRC Oxford Institute for Radiation Oncology, Great Britain</i>
Christoph Bert	<i>FAU Erlangen-Nürnberg, UK Erlangen, Germany</i>
Till Tobias Böhlen	<i>EBG MedAustron GmbH, Wr. Neustadt, Austria</i>
Stephanie Combs	<i>Klinikum rechts der Isar, TU München, Germany</i>
Anna Constantinescu	<i>GSI Helmholtzzentrum für Schwerionenforschung, Darmstadt, Germany</i>
Stefanie Ehrbar	<i>University Hospital Zurich, Switzerland</i>
Frank Emert	<i>Paul Scherrer Institute, Villigen, Switzerland</i>
Wolfgang Enghardt	<i>OncoRay, Dresden, Germany</i>
Giovanni Fattori	<i>Paul Scherrer Institute, Villigen, Switzerland</i>
Yusuke Fujii	<i>Hokkaido University, Japan</i>
Hugo Furtado	<i>Medical University of Vienna, Austria</i>
Orçun Göksel	<i>ETH Zurich, Switzerland</i>
Christian Graeff	<i>GSI Helmholtzzentrum für Schwerionenforschung, Darmstadt, Germany</i>
David Hawkes	<i>University College London, Great Britain</i>
Mischa Hoogeman	<i>Erasmus MC / HollandPTC, Netherlands</i>
Hiraku Iramina	<i>Graduate School of Engineering, Kyoto University, Japan</i>
Annika Jakobi	<i>OncoRay, Dresden, Germany</i>
Jürgen Jenne	<i>Fraunhofer MEVIS, Heidelberg, Germany</i>
Christoph Jud	<i>University of Basel, Switzerland</i>
Antje Knopf	<i>ICR / RMH, London, Great Britain</i>
Erik Korevaar	<i>UMC Groningen, Netherlands</i>
Gabriele Kragl	<i>EBG MedAustron GmbH, Wr. Neustadt, Austria</i>
Christopher Kurz	<i>Ludwig-Maximilians-University Munich, Germany</i>
Stephanie Lang	<i>University Hospital Zurich, Switzerland</i>
Tony Lomax	<i>Paul Scherrer Institute, Villigen, Switzerland</i>
Daniel Low	<i>University of California, Los Angeles, United States of America</i>
Philipp Mann	<i>German Cancer Research Center (DKFZ), Heidelberg, Germany</i>
Taeko Matsuura	<i>Hokkaido University, Japan</i>
Martin Menten	<i>The Institute of Cancer Research, London, Great Britain</i>
Nadia Möri	<i>University of Basel, Switzerland</i>
Ludvig Muren	<i>Aarhus University Hospital, Denmark</i>
Mitsuhiro Nakamura	<i>Kyoto University Hospital, Japan</i>
Tinsu Pan	<i>M.D. Anderson Cancer Center, Houston, United States of America</i>

Katia Parodi *Ludwig-Maximilians-University Munich, Germany*  
 Guntram Pausch *OncoRay, Dresden, Germany*  
 Andrea Pella *Politecnico di Milano, Italy*  
 Rosalind Perrin *Paul Scherrer Institute, Villigen, Switzerland*  
 Jørgen Petersen *Aarhus University Hospital, Denmark*  
 Tina Pfeiler *Westdeutsches Protonentherapiezentrum Essen (WPE), Germany*  
 Per Poulsen *Aarhus University Hospital, Denmark*  
 Anne Richter *University of Wuerzburg, Germany*  
 Christian Richter *OncoRay, Dresden, Germany*  
 Ilaria Rinaldi *Institut de Physique Nucleaire de Lyon, France*  
 Antoni Rucinski *Istituto Nazionale di Fisica Nucleare (INFN), Roma, Italy*  
 Nami Saito *German Cancer Research Center (DKFZ), Heidelberg, Germany*  
 Oliver Schrenk *German Cancer Research Center (DKFZ), Heidelberg, Germany*  
 Marco Serpa *University Hospital Erlangen, Germany*  
 Shinichi Shimizu *Hokkaido University, Japan*  
 Thilo Sothmann *University Medical Center Hamburg-Eppendorf, Germany*  
 Camilla Stokkevåg *Haukeland University Hospital, Bergen, Norway*  
 Kristin Stützer *OncoRay, Dresden, Germany*  
 Christine Tanner *ETH Zurich, Switzerland*  
 Nadine Traulsen *Fraunhofer MEVIS, Lübeck, Germany*  
 Fred Ubbels *UMC Groningen, Netherlands*  
 Riccardo Via *Politecnico di Milano, Italy*  
 Samatha Warren *CRUK/MRC Oxford Institute for Radiation Oncology, Great Britain*  
 Damien Charles Weber *Paul Scherrer Institute, Villigen, Switzerland*  
 Moritz Wolf *GSI Helmholtzzentrum für Schwerionenforschung, Darmstadt, Germany*  
 Ye Zhang *Paul Scherrer Institute, Villigen, Switzerland*

### **... FROM INDUSTRY DEPARTMENTS**

Franco Canestri *C-RAD GmbH, Karlsruhe, Germany*  
 Frederic Dessy *IBA, Louvain-La-Neuve, Belgium*  
 Erik Engwall *RaySearch Laboratories, Stockholm, Sweden*  
 Matthias Fippel *Brainlab AG, Feldkirchen, Germany*  
 Rui Galhos *ELEKTA, Crawley, United Kingdom*  
 Isabel Huth *Varian Medical Systems Particle Therapy GmbH, Troisdorf, Germany*  
 Johann Kindlein *Medinex GmbH, Adendorf, Germany*  
 Masumi Umezawa *Hitachi, Ltd, Tokyo, Japan*

